Resilience assessment under imprecise probability

Cao Wang, Ph.D., M.ASCE[1], Michael Beer, Dr.Eng., M.ASCE[2],
Matthias G.R. Faes, Ph.D., M.ASCE[3], and De-Cheng Feng, Ph.D., M.ASCE[4]

ABSTRACT

Resilience analysis of civil structures and infrastructure systems is a powerful approach to quantifying the object's ability to prepare for, recovery from and adapt to disruptive events. The resilience is typically measured probabilistically by the integration of the time-variant performance function, which is by nature a stochastic process as it is affected by many uncertain factors such as the hazard occurrences and the post-hazard recoveries. Resilience evaluation could be challenging in many cases with imprecise probability information on the time-variant performance function. In this paper, a novel method for the assessment of imprecise resilience is presented, which deals with resilience problems with non-probabilistic performance function. The proposed method, producing lower and upper bounds for the imprecise resilience, has benefited from that for imprecise reliability as documented in the literature, motivated by the similarity between reliability and resilience. Two types of stochastic processes, namely log-Gamma and lognormal processes, are employed to model the performance function, with which the explicit form of resilience is derived. Moreover, for a planning horizon within which the hazards may occur for multiple times, the incompletely-informed performance function results in "time-dependent imprecise resilience", which is dependent on the duration of the service period (e.g., life-cycle), and can also be handled by applying the proposed method. Through examining the time-dependent resilience of a strip foundation in a coastal area subjected to groundwater intrusion in a changing climate, the applicability of the proposed resilience bounding method is demonstrated.

[1]Lecturer & Career Development Fellow, School of Civil, Mining, Environmental and Architectural Engineering, Univ. of Wollongong, Wollongong, NSW 2522, Australia (corresponding author). ORCID: http://orcid.org/0000-0002-2802-1394. Email: wangc@uow.edu.au

[2]Professor of Uncertainty in Engineering and Head, Institute for Risk and Reliability, Leibniz Univ. Hannover, Hannover 30167, Germany; Professor, Institute for Risk and Uncertainty, Univ. of Liverpool, Liverpool L69 7ZF, UK; Guest Professor, International Joint Research Center for Resilient Infrastructure & International Joint Research Center for Engineering Reliability and Stochastic Mechanics, Tongji Univ., Shanghai 200092, China.

[3]Professor, Chair for Reliability Engineering, TU Dortmund Univ., Dortmund 44137, Germany.

[4]Professor, Key Laboratory of Concrete and Prestressed Concrete Structures of the Ministry of Education, Southeast Univ., Nanjing 211189, China.

The impact of imprecise probability information on resilience is quantified through sensitivity analysis.

Keywords: Imprecise resilience; time-dependent resilience; performance function; imprecise information; resilience bounding; climate change.

INTRODUCTION

In-service civil structures and infrastructure systems are often subjected to severe environmental or operational attacks such as natural hazards. Reliability and resilience assessment are powerful tools to evaluate an object's ability to withstand disruptive events. The former focuses on the post-hazard state (failure or survival) of an object (Ellingwood 2005; Melchers and Beck 2018; Wang 2021b), while the latter (i.e., resilience) additionally considers the post-hazard recovery process (Bruneau et al. 2003; National Research Council 2012a; Bocchini et al. 2014). In the presence of the various sources of uncertainties arising from structural properties (e.g., strength and stiffness) and load effects, the identification of the probability distributions of random variables is a key step for reliability and resilience evaluation. However, in many cases, due to the availability of only limited data, it is difficult or even impossible to uniquely determine the probability distribution of a random variable but the low-order moments such as mean value and variance (Coolen 2004). Correspondingly, the incompletely-informed random variable is quantified by a family of possible probability distributions, which forms the concept of "imprecise probability" (Walley 2000; Beer et al. 2013; Augustin et al. 2014).

Probability bounding approaches have been widely used in the literature to construct envelopes for imprecise probability functions, including probability-box (p-box) (Ferson et al. 2003; Faes et al. 2021a), random set and Dempster-Shafer evidence theory (Wu et al. 2002; Limbourg and De Rocquigny 2010), and fuzzy sets (Dubois and Prade 1989; Kahraman et al. 2016). With these approaches, one can further determine the lower and upper bounds of "imprecise reliability" (Zhang 2012; Alvarez and Hurtado 2014; Utkin and Coolen 2007; Penmetsa and Grandhi 2002; Oberguggenberger and Fellin 2008; Zhang et al. 2010; Wu et al. 2016; Wang et al. 2018). For example, Zhang et al. (2010) proposed an interval Monte Carlo (MC) method to estimate the interval failure probability, by combining simulation process with interval analysis. Wang et al. (2018) proposed a linear programming (LP)-based method to solve reliability problems in the presence of one or multiple imprecise random variable(s). The method constructs linear constraints on the imprecise probability distribution by considering the known moments of the variables. Other recent developments in this context include the application of operator norm theory (Faes et al. 2020; Faes et al. 2021b), solving the imprecise probability problem in an augmented form (Zhang and Shields 2019; Wei et al. 2019; Faes et al. 2021c), and the use of Bayesian active learning (Dang et al. 2022).

The resilience of an object (e.g., a structure or system) is typically measured by the integration of performance function over time (Bruneau et al. 2003; Cimellaro et al. 2010; Attoh-Okine et al. 2009; Wang 2023). Due to the occurrence of a hazardous event, the object's performance degrades due to the hazard-induced damage, and may be restored to the pre-hazard state given the availability of resource. This indicates that the resilience is dependent on the factors influencing the time-variation of performance function (e.g., the occurrence time and intensity of hazards, and the post-hazard recovery processes), and thus should be evaluated in a probabilistic framework considering the uncertainties associated with these factors. In particular, for the case where imprecise variables are involved in the performance function, the resilience cannot be determined uniquely, but varies within an interval, and thus is called "imprecise resilience" in this paper. Furthermore, for a planning horizon, the resilience is dependent on the duration of the reference period, and is known as "time-dependent resilience" (Wang and Ayyub 2022). In this regard, the presence of imprecise information on the performance function over the service period of interest further leads to "time-dependent imprecise resilience". Similar to the evaluation of "imprecise reliability", the importance of determining an interval for imprecise resilience (featured by lower and upper bounds) is evident in the context of decision-making based on imprecise probabilities. This is usually the ultimate goal of resilience quantification. However, based on the current state-of-the-art, it is unclear how imprecise resilience measures have to be computed.

The novelty of this paper is therefore to propose a novel method to quantify the interval for imprecise resilience in the presence of a performance function that is subjected to epistemic uncertainty. The method benefits from the same formalism as used to in the field of imprecise reliability analysis, motivated by the similarity between reliability and resilience from a mathematical perspective.

Two types of stochastic processes for performance function are used in the quantification of imprecise resilience, namely log-Gamma and lognormal processes. An example is presented to demonstrate the applicability of the proposed bounding techniques for imprecise resilience by examining the life-cycle resilience of a strip foundation located in a coastal area subjected to groundwater intrusion. The role of incomplete probability information on the performance deterioration and climate change scenarios in resilience is investigated. The scope of this paper is related to the United Nations (UN) Sustainable Development Goal (SDG) 11 "Make cities and human settlements inclusive, safe, resilient and sustainable".

RESILIENCE MEASURE

The performance function/quality of an object (e.g., a structure, or a system consisting of multiple structures) is a key component in resilience assessment. For example, Bruneau et al. (2003) defined "loss of resilience" as $\int_{t_0}^{t_1}[100\% - Q(t)]dt$, in which t_0 is the occurrence time of a disruptive event, t_1 is the time to recovery, and $Q(t)$ is the time-variant performance function (taking a value between 0 and 100%). Further, a dimensionless measure for resilience, denoted by R_e, is as follows (Attoh-Okine et al. 2009; Cimellaro et al. 2010),

$$R_e = \frac{1}{t_h - t_0}\int_{t_0}^{t_h} Q(t)dt \tag{1}$$

where t_h is a reference time (e.g., it may refer to the time to full recovery, t_1). Note that the resilience model in Eq. (1) has been based on the arithmetic mean of the performance function over $[t_0, t_h]$, and thus is insensitive to the variation of $Q(t)$, in particular for an extremely small value of performance function. With this regard, a generalized resilience measure was proposed by Wang (2023), taking a form of the following,

$$R_e = f^{-1}\left[\frac{1}{t_h - t_0}\int_{t_0}^{t_h} f[Q(t)]dt\right] \tag{2}$$

in which f is a generating function. If $f(x) = x$, then Eq. (2) reduces to (1). If $f(x) = \ln x$, Eq. (2) becomes,

$$R_e = \exp\left[\frac{1}{t_h - t_0}\int_{t_0}^{t_h} \ln[Q(t)]dt\right] \tag{3}$$

It can be verified that, the resilience in Eq. (3) has been based on the geometric mean of $Q(t)$ over $[t_0, t_h]$, and thus can better reflect the sensitivity of resilience to the variation of performance function. Note that in Eq. (3), the resilience is a random variable because $Q(t)$ is a stochastic process. In order to achieve a scalar measure for resilience, the mean value of R_e in Eq. (3) will be considered, which is denoted by $\overline{R}_e$ and is expressed as follows,

$$\overline{R}_e = \mu\left\{\exp\left[\frac{1}{t_h - t_0}\int_{t_0}^{t_h} \ln[Q(t)]dt\right]\right\} \tag{4}$$

in which $\mu()$ denotes the mean value of the variable in the brackets. The resilience model in Eq. (4) establishes a unified framework for reliability and resilience (Wang 2023). One example is presented in Fig. 1(a), where a hazardous event occurs at time t_0, causing the reduction of $Q(t)$ until time t_f ($t_f \geq t_0$). In particular,

Fig. 1(a1) focuses on the resilience problem, where the reduced $Q(t)$ is restored to a pre-hazard state from time t_f until time t_r. In the context of reliability, however, the focus is on a survival-or-failure state without considering the post-hazard recovery process. As illustrated in Fig. 1(a2), the performance function $Q(t) \equiv 1$ within $[t_f, t_r]$ if the object survives, and $Q(t) \equiv 0, t \in [t_f, t_r]$ in the presence of a failure state. Let random variables A and B be R_e in Eq. (3) with t_h being replaced by t_r, corresponding to the scenarios in Figs. 1(a1) and (a2), respectively. Clearly, $A \in [0, 1]$ and $B \in \{0, 1\}$. The mean resilience (see Eq. (4)) and reliability (denoted by R_l) are determined as $\mu(A)$, and $\mu(B)$, respectively. This indicates the inherent similarity between resilience and reliability as both quantities can be obtained through the performance function of an object.

The resilience model in Eq. (4) will be adopted in this paper. One can further extend Eq. (4) to handle resilience problems over other reference periods by replacing the time interval $[t_0, t_h]$. For example, the time-dependent resilience over a life cycle of $[0, t_l]$ (within which the disruptive events may occur for multiple times), denoted by $\overline{R}_e(0, t_l)$, is as follows,

$$\overline{R}_e(0, t_l) = \mu \left\{ \exp \left[\frac{1}{t_l} \int_0^{t_l} \ln[Q(t)] dt \right] \right\} \tag{5}$$

Similar to Fig. 1(a), the comparison between time-dependent resilience and time-dependent reliability is demonstrated in Fig. 1(b) based on Eq. (5), considering two hazardous events occurring at times t_{01} and t_{02}, respectively. In the context of resilience as in Fig. 1(b1), the first disruptive event results in the performance function degrading from 1 to q at time t_{f1}, followed by a recovery process until time t_{r1} ($t_{r1} < t_{02}$). However, due to the second hazard, the object collapses and no recovery follows. Let A_1 and A_2 be the resilience associated with the two hazardous events, respectively, which are evaluated as follows,

$$A_1 = \exp \left[\frac{1}{t_l} \int_{t_{01}}^{t_{r1}} \ln[Q(t)] dt \right], \quad A_2 = \exp \left[\frac{1}{t_l} \int_{t_{02}}^{t_l} \ln[Q(t)] dt \right] \tag{6}$$

With this, the resilience over $[0, t_l]$, denoted by A_{12}, equals $A_1 \cdot A_2$, by noting that,

$$\begin{aligned} A_{12} &= \exp \left[\frac{1}{t_l} \int_0^{t_l} \ln[Q(t)] dt \right] \\ &= \exp \left[\frac{1}{t_l} \int_0^{t_{01}} \ln[Q(t)] dt \right] \cdot A_1 \cdot \exp \left[\frac{1}{t_l} \int_{t_{r1}}^{t_{02}} \ln[Q(t)] dt \right] \cdot A_2 \\ &= A_1 \cdot A_2 \end{aligned} \tag{7}$$

In particular, if $A_2 = 0$, then $A_{12} = 0$, implying that the object is not resilient in the presence of zero resilience associated with any hazardous event.

In terms of reliability, as shown in Fig. 1(b2), a Bernoulli variable B_i ($i = 1, 2$) is introduced to denote the state (either survival or failure) associated with the ith disruptive event ($B_i = 1$ for "survival" and $B_i = 0$ for "failure"). The state for the whole life-cycle is then equal to $B_1 \cdot B_2$, which is similar to the relationship in Eq. (7).

The observations from Fig. 1 demonstrate that Eq. (4) provides a general framework for the evaluation of resilience and reliability. This further motivates the generalization of existing approaches in the literature for imprecise reliability to handle imprecise resilience, as will be discussed in the next section.

BOUNDS FOR RESILIENCE IN THE PRESENCE OF IMPRECISE PROBABILITY INFORMATION

Problem formulation

Consider a resilience problem involving totally N_X imprecise random variables ($X_1, X_2, \ldots X_{N_X}$) and N_Y ordinary (probabilistic) random variables $Y_1, Y_2, \ldots Y_{N_Y}$. The mean resilience is expressed by a function ψ as follows,

$$\overline{R}_e = \mu\left[\psi(\mathbf{X}, \mathbf{Y})\right] \tag{8}$$

in which $\mathbf{X} = \{X_1, X_2, \ldots, X_{N_X}\}$ and $\mathbf{Y} = \{Y_1, Y_2, \ldots, Y_{N_Y}\}$. Note that Eq. (8) should be interpreted as $\overline{R}_e$ being a function of the imprecise random variables $\mathbf{X}$, where a crisp value of $\overline{R}_e$ is obtained for each realization of the epistemic uncertainty in $\mathbf{X}$. Herein, the imprecise random variables $\mathbf{X}$ are described by a family of distributions $\mathfrak{F}$ according to the respective model used to describe the imprecise probability.

For ψ, one can use Eq. (4) to evaluate the resilience associated with a single event, or Eq. (5) for the time-dependent resilience over $[0, t_l]$. Due to the epistemic uncertainty that is present in $\mathbf{X}$, one cannot determined the resilience in Eq. (8) uniquely. Instead, $\overline{R}_e$ will vary within in interval, which is dependent on "how precise the information on $\mathbf{X}$ is". As an example, consider for instance that $\mathbf{X}$ is described by a parametric family of normal distributions according to,

$$\mathfrak{F} = \left\{F_X(., \boldsymbol{\vartheta}) \mid F_X(., \boldsymbol{\vartheta}) \in \mathbb{F}, \boldsymbol{\vartheta} \in \left[\mu_{X,\mathrm{lb}}, \mu_{X,\mathrm{ub}}\right] \times \left[\sigma_{X,\mathrm{lb}}, \sigma_{X,\mathrm{ub}}\right]\right\}, \tag{9}$$

where $\mathbb{F}$ is the family of normal distribution functions, $\mu_{X,\mathrm{lb}}$, $\mu_{X,\mathrm{ub}}$ are the lower and upper bounds of the mean value of X, and $\sigma_{X,\mathrm{lb}}$, $\sigma_{X,\mathrm{ub}}$ are the lower and upper bounds of the standard deviation of X. As such, every realisation of $\boldsymbol{\vartheta}$ will yield a precise value for $\overline{R}_e$, without providing any distributional information on the quantity. It is assumed that dF_X/dx exists.

The aim of the rest of this section is to address techniques to determine the bounds $\overline{R}_e$, which will benefit from those in the literature for imprecise reliability. Denote

$$\theta(\mathbf{X}) = \int \dots \int \psi(\mathbf{X}, \mathbf{Y}) f_{\mathbf{Y}}(\mathbf{y}) d\mathbf{y}, \tag{10}$$

in which $f_{\mathbf{Y}}(\mathbf{y})$ is the joint probability distribution function (PDF) of $\mathbf{Y}$. With this, Eq. (8) becomes,

$$\overline{R}_e = \int \dots \int \theta(\mathbf{x}) f_{\mathbf{X}}(\mathbf{x}) d\mathbf{x}, \tag{11}$$

where $f_{\mathbf{X}}(\mathbf{x})$ is the joint PDF of $\mathbf{X}$. It is assumed that each X_i is statistically independent, with which,

$$f_{\mathbf{X}}(\mathbf{x}) = \prod_{i=1}^{N_X} f_{X_i}(x_i), \tag{12}$$

in which $f_{X_i}(x)$ is the PDF of X_i. This condition is assumed to hold for every realisation of the epistemic uncertainty.

Due to the imprecise information on $\mathbf{X}$, the explicit form of $f_{\mathbf{X}}(\mathbf{x})$ is only known up to a set description. Therefore, one can only evaluate Eq. (11) numerically for each realisation of the epistemic uncertainty in $\mathbf{X}$. Further, the following two optimization problems can be solved to find the lower and upper bounds of $\overline{R}_e$, denoted by $\overline{R}_{e,\mathrm{lb}}$ and $\overline{R}_{e,\mathrm{ub}}$ respectively,

$$\overline{R}_{e,\mathrm{lb}} = \min_{f_{\mathbf{X}} \in \mathfrak{F}} \int \dots \int \theta(\mathbf{x}) f_{\mathbf{X}}(\mathbf{x}) \, \mathrm{d}\mathbf{x}, \tag{13}$$

and

$$\overline{R}_{e,\mathrm{ub}} = \max_{f_{\mathbf{X}} \in \mathfrak{F}} \int \dots \int \theta(\mathbf{x}) f_{\mathbf{X}}(\mathbf{x}) \, \mathrm{d}\mathbf{x}. \tag{14}$$

A special case of Eqs. (13) and (14) is the case where there exists θ_{lb} and θ_{ub} satisfying

$$\theta_{\mathrm{lb}} = \min_{\mathbf{x}} \theta(\mathbf{x}), \quad \theta_{\mathrm{ub}} = \max_{\mathbf{x}} \theta(\mathbf{x}) \tag{15}$$

with which it follows that,

$$\theta_{\text{lb}} \leq \overline{R}_e \leq \theta_{\text{ub}} \tag{16}$$

Note that in a more general setting, these optimization problems are potentially very complicated since the optimization has to be carried out over the set of all possible $f_{\mathbf{X}}$ consistent with the definition of the family of distributions $\mathfrak{F}$. Hence, this constitutes a non-convex, discontinuous optimization problem, which are notoriously difficult so solve exactly. In this regard, two bounding methods for $\overline{R}_e$ will be discussed in the following, namely interval MC method and LP-based method. For a more general treatment of the topic in the context of reliability engineering, the reader is referred to Faes et al. (2021a) for an overview.

Interval Monte Carlo method

The interval MC method, which has been successfully applied in the evaluation of imprecise reliability (Zhang et al. 2010), is used herein to determine the lower and upper bounds of $\overline{R}_e$ in Eq. (11). With this regard, the imprecise cumulative distribution function (CDF) of $\mathbf{X}$ is first represented by a p-box. Let F_X be the CDF of a random variable X (it can be replaced by $X_1, X_2, \ldots, X_{N_X}$ in Eq. (11)), which is bounded by an envelope as follows,

$$F_{X,\text{lb}}(x) \leq F_X(x) \leq F_{X,\text{ub}}(x), \quad \text{for } \forall x \tag{17}$$

where $F_{X,\text{lb}}$ and $F_{X,\text{ub}}$ are the lower and upper bounds of F_X respectively, which are dependent on the available information on X. For example, if the mean (μ_X) and standard deviation (σ_X) of X are known, Oberguggenberger and Fellin (2008) applied the Chebyshev's inequality to derive $F_{X,\text{lb}}$ and $F_{X,\text{ub}}$ as follows,

$$F_{X,\text{lb}}(x) = \begin{cases} 0, & x \leq \mu_X + \sigma_X \\ 1 - \dfrac{\sigma_X^2}{(x-\mu_X)^2}, & x \geq \mu_X + \sigma_X \end{cases} \tag{18a}$$

$$F_{X,\text{ub}}(x) = \begin{cases} \dfrac{\sigma_X^2}{(x-\mu_X)^2}, & x \leq \mu_X - \sigma_X \\ 1, & x \geq \mu_X - \sigma_X \end{cases} \tag{18b}$$

If it is additionally known that X varies within an interval of $[x_{\text{lb}}, x_{\text{ub}}]$, then an updated set of $F_{X,\text{lb}}, F_{X,\text{ub}}$ is (Faes et al. 2021a),

$$F_{X,\text{lb}}(x) = \begin{cases} 0, & x \leq \mu_X + \sigma_X^2/(\mu_X - x_{\text{ub}}) \\ 1 - [b(1+a) - c - b^2]/a, & \mu_X + \sigma_X^2/(\mu_X - x_{\text{ub}}) < x < \mu_X + \sigma_X^2/(\mu_X - x_{\text{lb}}) \\ 1/[1 + \sigma_X^2/(x - \mu_X)^2], & \mu_X + \sigma_X^2/(\mu_X - x_{\text{lb}}) \leq x < x_{\text{ub}} \\ 1, & x \geq x_{\text{ub}} \end{cases} \tag{19a}$$

$$F_{X,\text{ub}}(x) = \begin{cases} 0, & x \leq x_{\text{lb}} \\ 1/[1 + (x - \mu_X)^2/\sigma_X^2], & x_{\text{lb}} \leq x < \mu_X + \sigma_X^2/(\mu_X - x_{\text{ub}}) \\ 1 - (b^2 - ab + c)/(1-a), & \mu_X + \sigma_X^2/(\mu_X - x_{\text{ub}}) < x < \mu_X + \sigma_X^2/(\mu_X - x_{\text{lb}}) \\ 1, & x \geq \mu_X + \sigma_X^2/(\mu_X - x_{\text{lb}}) \end{cases} \tag{19b}$$

where $a = (x - x_{\text{lb}})/(x_{\text{ub}} - x_{\text{lb}})$, $b = (\mu_X - x_{\text{lb}})/(x_{\text{ub}} - x_{\text{lb}})$, and $c = \sigma_X^2/(x_{\text{ub}} - x_{\text{lb}})^2$.

The CDF envelope in Eq. (17) for X enables the use of MC simulation to find the bounds of $\overline{R}_e$. For the jth simulation run ($j = 1, 2, \ldots, N$), two vector samples, $\mathbf{x}_{j,\text{lb}} = [x_{1j,\text{lb}}, x_{2j,\text{lb}}, \ldots, x_{N_X j,\text{lb}}]$ and $\mathbf{x}_{j,\text{ub}} = [x_{1j,\text{ub}}, x_{2j,\text{ub}}, \ldots, x_{N_X j,\text{ub}}]$, are first generated based on the bounds of F_{X_i}, respectively, according to

$$u_{ij} = F_{X_i,\text{ub}}(x_{ij,\text{lb}}) = F_{X_i,\text{lb}}(x_{ij,\text{ub}}) \tag{20}$$

in which u_{ij} is a sample of uniform distribution within $[0, 1]$ for the jth simulation and the ith imprecise variable, $i = 1, 2, \ldots, N_X$, and $j = 1, 2, \ldots, N$. In such a way, the interval $[\mathbf{x}_{j,\text{lb}}, \mathbf{x}_{j,\text{ub}}]$ contains all the possible realizations of $\mathbf{X}$. Let $\min \theta\left(\mathbf{x}_j\right)$ and $\max \theta\left(\mathbf{x}_j\right)$ respectively be the minimum and maximum of $\theta(\mathbf{x}_j)$ subjected to $\mathbf{x}_{j,\text{lb}} \leq \mathbf{x}_j \leq \mathbf{x}_{j,\text{ub}}$. With this, one has,

$$\underbrace{\frac{1}{N}\sum_{j=1}^{N} \min \theta\left(\mathbf{x}_j\right)}_{\text{Lower bound: } \overline{R}_{e,\text{lb}}} \leq \frac{1}{N}\sum_{j=1}^{N} \theta(\mathbf{x}_j) \leq \underbrace{\frac{1}{N}\sum_{j=1}^{N} \max \theta\left(\mathbf{x}_j\right)}_{\text{Upper bound: } \overline{R}_{e,\text{ub}}} \tag{21}$$

which gives the expressions for the lower and upper bound of $\overline{R}_e$, denoted by $\overline{R}_{e,\text{lb}}$ and $\overline{R}_{e,\text{ub}}$, respectively.

Linear programming-based method

An LP-based method was previously proposed by Wang et al. (2018) to determine the bounds of imprecise reliability in the presence of one or more imprecise random variables (with unknown CDF but known moments). This method will be adopted herein to handle the imprecise resilience problem. First, consider the case with a single imprecise variable, denoted by X, whose mean value (μ_X) and standard deviation (σ_X) are known only. With this, Eq. (11) is rewritten as follows,

$$\overline{R}_e = \int \theta(x) f_X(x) dx \tag{22}$$

Assume that X varies within $[x_{\min}, x_{\max}]$. If no information on $x_{\min}$ and $x_{\max}$ is available, the two bounds can be practically assigned as $\mu_X \pm \kappa\sigma_X$ with a sufficiently large κ (e.g., $\kappa = 5$). A new variable Z is introduced, which is a normalization of X and is defined as

$$Z = \frac{X - x_{\min}}{x_{\max} - x_{\min}} \tag{23}$$

Correspondingly, Eq. (22) becomes

$$\overline{R}_e = \int_0^1 \theta_Z(z) f_Z(z) dz \tag{24}$$

in which $\theta_Z(z) = \theta((x_{\max} - x_{\min})z + x_{\min})$, and $f_Z(z)$ is the PDF of Z. Since $Z \in [0, 1]$, the domain of Z is subdivided into n identical sections (where n is a sufficiently large integer), namely $[0, 1/n]$, $[1/n, 2/n]$, $\ldots [(n-1)/n, 1]$. With this, the PDF of Z is approximated by a sequence of $\{f_{Z,i}\}, i = 1, 2 \ldots n$, where $f_{Z,i} = f_Z((i - 0.5)/n)$. Thus, Eq. (24) is rewritten as follows from a view of Riemann integral,

$$\overline{R}_e = \int_0^1 \theta_Z(z) f_Z(z) dz = \sum_{i=1}^{n} \theta_Z\left(\frac{i-0.5}{n}\right) \frac{1}{n} \cdot f_{Z,i} \tag{25}$$

Since the mean value (μ_Z) and standard deviation (σ_Z) of Z are known based on μ_X and σ_X, one can construct the following constraints on $\{f_{Z,i}\}$,

$$\begin{cases} \sum_{i=1}^{n} f_{Z,i} \cdot \frac{1}{n} = 1 \\ \sum_{i=1}^{n} f_{Z,i} \cdot \frac{1}{n} \cdot \frac{i}{n} = \mu_Z \\ \sum_{i=1}^{n} f_{Z,i} \cdot \frac{1}{n} \left(\frac{i}{n}\right)^2 = \mu_Z^2 + \sigma_Z^2 \\ 0 \le f_{Z,i} \le n, \forall i = 1, 2, \ldots n \end{cases} \tag{26}$$

Based on Eqs. (25) and (26), the bounds for $\overline{R}_e$ can be determined through an LP-based method. The object is to maximize (for the upper bound of $\overline{R}_e$) or minimize (for the lower bound) $\overline{R}_e$ in Eq. (25) with respect to $\{f_{Z,i}\}$, while the constraints on $\{f_{Z,i}\}$ are presented in Eq. (26).

Recall that only one imprecise random variable has been involved in Eq. (22). One can extend the LP-based method to solve the imprecise resilience problem with N_X imprecise variables ($N_X \ge 2$) in Eq. (11). This is similar to the reliability bounding technique in Wang et al. (2018) considering multiple imprecise variables using LP.

Eq. (11) indicates that $\overline{R}_e$ is dependent on each PDF f_{X_i} with a fixed $\theta(\mathbf{x})$. Thus, Eq. (11) is expressed as follows with an emphasis on the dependence of $\overline{R}_e$ on each f_{X_i},

$$\overline{R}_e = \zeta(f_{X_1}(x_1), f_{X_2}(x_2), \ldots, f_{X_{N_X}}(x_{N_X})) \tag{27}$$

Denote $\mathfrak{F}_{X_i}$ the set of possible candidate PDFs of X_i. An iteration-based approach is used to find the bound of $\overline{R}_e$, as summarized in the following. Let ϵ be a predefined error limit (say, 10^{-5}) for the iteration process, and $f_{X_i,j}$ the PDF of X_i associated with the jth iteration, $j = 1, 2, \ldots$.

1. Allocate initial PDFs for each X_i (e.g., normal distribution), denoted by $f_{X_1,1}$ through to $f_{X_{N_X},1}$, and calculate $\zeta_1 = \zeta(f_{X_1,1}, f_{X_2,1}, \ldots, f_{X_{N_X},1})$.
2. For $j = 2$, and $i = 1, 2, \ldots N_X$, repeatedly find $f_{X_i,j} \in \mathfrak{F}_{X_i}$ that maximizes (for the upper bound of $\overline{R}_e$) or minimizes (for the lower bound) the following item based on Eqs. (25) and (26),

$$\zeta(f_{X_1,j}, f_{X_2,j}, \ldots, f_{X_{i-1},j}, \underbrace{f_{X_i,j}}_{\text{to be optimized}}, \ldots, f_{X_{i+1},j-1}, \ldots, f_{X_{N_X},j-1}),$$

and compute $\zeta_j = \zeta(f_{X_1,j}, f_{X_2,j}, \ldots, f_{X_{N_X},j})$.

3. In Step 2, if $|\zeta_j - \zeta_{j-1}| \le \epsilon$, then ζ_j is determined as the (lower or upper) bound of $\overline{R}_e$; otherwise,

return to Step 2 with j replaced by $j+1$.

The convergence of the above iteration-based approach was proven in Wang et al. (2018).

BOUNDS OF RESILIENCE BASED ON IMPRECISE PERFORMANCE FUNCTION

Explicit expression of resilience

Two bounding techniques have been discussed above to determine the lower and upper bounds of the imprecise resilience in Eq. (8). It has been demonstrated that the availability of probability information on the (imprecise) random variables is a key element in finding the resilience bounds. On the other hand, the explicit expression of $\overline{R}_e$ as a function of the involved variables ($\mathbf{X}$ and $\mathbf{Y}$) serves as the foundation for the bounding techniques. As revealed in Eq. (4), the resilience is dependent on the time-variant performance function $Q(t)$, which is by nature a stochastic process. To reflect the uncertainty associated with $Q(t)$, one would need to employ appropriate stochastic processes to model $Q(t)$, based on which the explicit expression of $\overline{R}_e$ can be derived. In this paper, two types of (imprecise) processes will be considered for $Q(t)$, namely log-Gamma and lognormal, as will be addressed in the next two sections. Theoretically, also more general formulations such as distribution-free imprecise processes (Faes et al. 2022) can be applied. This is left for future work.

For many resilience problems, the use of a single type of stochastic process is insufficient to describe $Q(t)$. For example, as shown in Fig. 1(a1), $Q(t)$ decreases first from t_0 to t_f, followed by a recovery process from t_f to t_r. In such a case, it is reasonable to model $Q(t)$ using two stochastic processes for the periods of $[0, t_f]$ and $[t_f, t_r]$, respectively. Based on Eq. (4) with $t_h = t_r$, one has,

$$\overline{R}_e = \mu\left\{\exp\left[\frac{1}{t_r - t_0}\int_{t_0}^{t_f} \ln[Q(t)]dt\right] \cdot \exp\left[\frac{1}{t_r - t_0}\int_{t_f}^{t_r} \ln[Q(t)]dt\right]\right\} \tag{28}$$

Assume that the performance function within $[t_0, t_f]$ and that within $[t_f, t_r]$ are statistically independent, as they are associated with different mechanisms. With this, Eq. (28) is rewritten as follows,

$$\overline{R}_e = \underbrace{\mu\left\{\exp\left[\frac{1}{t_r - t_0}\int_{t_0}^{t_f} \ln[Q(t)]dt\right]\right\}}_{\text{Sub-problem 1}} \cdot \underbrace{\mu\left\{\exp\left[\frac{1}{t_r - t_0}\int_{t_f}^{t_r} \ln[Q(t)]dt\right]\right\}}_{\text{Sub-problem 2}} \tag{29}$$

Eq. (29) demonstrates that, the resilience for a reference period of $[t_0, t_r]$ can be evaluated by integrating those over $[t_0, t_f]$ and $[t_f, t_r]$, respectively (see Sub-problems 1 and 2 in Eq. (29)). In such a case, within each sub-interval, $Q(t)$ can be described by an independent stochastic process. Further, one can extend the service period of $[t_0, t_r]$ in Eq. (29) to $[0, t_l]$ to account for time-dependent resilience.

Log-Gamma process-based performance function

For a sub-interval within which the performance function decreases monotonically (e.g., the interval of $[t_0, t_f]$ in Fig. 1(a1)), one can employ a log-Gamma process to describe $Q(t)$. Mathematically, for $t \in [t_\mathrm{a}, t_\mathrm{b}] = [t_\mathrm{a}, t_\mathrm{a} + \delta_1]$, $Q(t)$ is expressed as follows,

$$Q(t) = \exp(-X(t)), \quad \text{with } Q(t_\mathrm{a}) = 1 \tag{30}$$

in which $X(t)$ is a Gamma process. The process $Q(t)$ in Eq. (30) is named a "log-Gamma" process because the logarithm of $Q(t)$ is a Gamma process up to a multiplicative scaling factor (the factor equals -1 in Eq. (30)).

For any $t^* \in [t_\mathrm{a}, t_\mathrm{b}]$, $X(t^*)$ (i.e., $X(t)$ evaluated at time t^*) follows a Gamma distribution with a shape parameter of $a(t^*) > 0$ and a scale parameter of $b > 0$, and is written as $X(t^*) \sim \mathrm{Ga}(a(t^*), b)$. The PDF of $X(t^*)$, denoted by $f_{X(t^*)}(x)$, is as follows,

$$f_{X(t^*)}(x) = \frac{(x/b)^{a(t^*)-1}}{b\Gamma(a(t^*))} \exp(-x/b), \quad x \geq 0 \tag{31}$$

where $\Gamma()$ is the Gamma function. With Eq. (31), the moment generating function (MGF) of $X(t^*)$ is (Ross 2014)

$$\psi_{X(t^*)}(\tau) = \mu[\exp(X(t^*)\tau)] = (1 - b\tau)^{-a(t^*)} \tag{32}$$

The Gamma process $X(t)$ in Eq. (30) is a continuous stochastic process with statistically independent and Gamma-distributed increments over time (Kahle et al. 2016). That is, for time instants $t_\mathrm{a} \leq t_0^* < t_1^* < \ldots < t_n^* \leq t_\mathrm{b}$, the variables $X(t_0^*) - X(t_\mathrm{a}), X(t_1^*) - X(t_0^*), \ldots X(t_n^*) - X(t_{n-1}^*)$ are independent of each other, and follow a Gamma distribution. Thus, $X(t)$ monotonically increases with t, with which $Q(t)$ in Eq. (30) is a decreasing stochastic process. In such a way, the uncertainty and monotonicity associated with the performance function within $[t_\mathrm{a}, t_\mathrm{b}]$ can be reflected through Eq. (30).

Next, the resilience associated with the monotonically-decreasing $Q(t)$ within $[t_\mathrm{a}, t_\mathrm{b}]$ is derived, which is expressed as follows,

$$\overline{R}_{e,\mathrm{sub}} = \mu\left(\exp\left[-\frac{1}{t_{\mathrm{ref}}}\int_{t_{\mathrm{a}}}^{t_{\mathrm{b}}} X(t)dt\right]\right) \tag{33}$$

Note that in Eq. (33), the subscript "sub" indicates that it is a sub-problem of resilience evaluation over a reference period with a duration of t_{ref} (see, e.g., Eq. (29) for explanation). For the resilience problem in Eq. (4), $t_{\mathrm{ref}} = t_h - t_0$. If the time-dependent resilience over the life cycle $[0, t_l]$ is considered, then t_{ref} equals t_l.

Denote $\widetilde{X}(t) \equiv X(t+t_{\mathrm{a}})$, and $\widetilde{a}(t) \equiv a(t+t_{\mathrm{a}})$. From a view of Riemann integral, discretizing the interval $[t_{\mathrm{a}}, t_{\mathrm{b}}]$ into n identical sections (n is sufficiently large), Eq. (33) is approximated by the following,

$$\overline{R}_{e,\mathrm{sub}} = \mu\left(\exp\left[-\frac{1}{t_{\mathrm{ref}}}\int_{0}^{\delta_1} \widetilde{X}(t)dt\right]\right) = \mu\left(\exp\left[-\frac{\delta_1}{t_{\mathrm{ref}}}\cdot\frac{1}{\delta_1}\sum_{i=1}^{n}\widetilde{X}_i\Delta t\right]\right) \tag{34}$$

where $\Delta t = \delta_1/n$, $\widetilde{X}_i = \widetilde{X}(t_i)$, and $t_i = i\delta_1/n$. Denote $\widetilde{X}_0 = 0$, and $\Delta_i = \widetilde{X}_i - \widetilde{X}_{i-1}$ for $i = 1, 2, \ldots n$. Due to the property of a Gamma process, Δ_i follows a Gamma distribution with a shape parameter of $\widetilde{a}'_i\Delta t$ and a scale parameter of b, where $\widetilde{a}'_i = \widetilde{a}'(t_i)$, and the symbol $'$ denotes the first order derivative of a function.

Since $\widetilde{X}_i = \sum_{j=1}^{i}\Delta_j$ for $i = 1, 2, \ldots n$, it follows that,

$$\overline{R}_{e,\mathrm{sub}} = \mu\left(\exp\left[-\frac{\delta_1}{t_{\mathrm{ref}}}\cdot\frac{\Delta t}{\delta_1}\sum_{i=1}^{n}(n+1-i)\Delta_i\right]\right) = \mu\left(\exp\left[-\frac{\delta_1}{t_{\mathrm{ref}}}\cdot\sum_{i=1}^{n}\Theta_i\right]\right) \tag{35}$$

in which $\Theta_i = (1 + (1-i)/n)\,\Delta_i$. Since $\Theta_i \sim \mathrm{Ga}\left(\widetilde{a}'_i\Delta t, (1+(1-i)/n)\,b\right)$, the MGF of Θ_i is

$$\psi_{\Theta_i}(\tau) = \mu(\exp(\tau\Theta_i)) = \left(1 - \left(1 + \frac{1-i}{n}\right)b\tau\right)^{-\widetilde{a}'_i\Delta t} \tag{36}$$

Further, by noting that each Θ_i is statistically independent (due to the independence of each Δ_i), the MGF of $\sum_i^n \Theta_i$ is

$$\psi_{\sum_{i=1}^{n}\Theta_i}(\tau) = \prod_{i=1}^{n}\psi_{\Theta_i}(\tau) = \prod_{i=1}^{n}\left(1 - \left(1 + \frac{1-i}{n}\right)b\tau\right)^{-\widetilde{a}'_i\Delta t} \tag{37}$$

With a sufficiently large n, one has,

$$\begin{aligned}\psi_{\sum_{i=1}^{n}\Theta_i}(\tau) &= \lim_{n\to\infty}\exp\left\{-\sum_{i=1}^{n}\ln\left(1-\left(1+\frac{1-i}{n}\right)b\tau\right)\widetilde{a}'_i\Delta t\right\}\\ &= \exp\left\{-\int_0^{\delta_1}\widetilde{a}'(t)\ln\left(1-\left(1-\frac{t}{\delta_1}\right)b\tau\right)dt\right\}\end{aligned} \tag{38}$$

Thus, $\overline{R}_{e,\text{sub}}$ in Eq. (35) is evaluated by

$$\overline{R}_{e,\text{sub}} = \psi_{\sum_{i=1}^{n}\Theta_i}\left(-\frac{\delta_1}{t_{\text{ref}}}\right) = \exp\left\{-\int_0^{\delta_1} \widetilde{a}'(t)\ln\left(1+\left(1-\frac{t}{\delta_1}\right)\frac{b\delta_1}{t_{\text{ref}}}\right)dt\right\} \tag{39}$$

Denote

$$\mathcal{H}(t) = \ln\left(1+\left(1-\frac{t}{\delta_1}\right)\frac{b\delta_1}{t_{\text{ref}}}\right) \tag{40}$$

Note that $\widetilde{a}(0) = 0$ and $\mathcal{H}(\delta_1) = 0$. Thus, Eq. (39) is rewritten as follows,

$$\overline{R}_{e,\text{sub}} = \exp\left\{-\int_0^{\delta_1}\mathcal{H}(t)d[\widetilde{a}(t)]\right\} = \exp\left\{-\frac{1}{t_{\text{ref}}}\int_0^{\delta_1}\widetilde{a}(t)\frac{b}{1+\left(1-\frac{t}{\delta_1}\right)\frac{b\delta_1}{t_{\text{ref}}}}dt\right\} \tag{41}$$

Eq. (41) presents an explicit formulation for the sub resilience problem in Eq. (33) in the presence of a log-Gamma performance function over $[t_{\text{a}}, t_{\text{b}}]$.

Next, a bias factor, η_{sub}, is introduced, which is defined as the ratio of resilience in Eq. (41) to that based on $\overline{Q}(t) = \mu(Q(t))$, denoted by $\overline{R}_{e,\text{sub},\overline{Q}}$. The factor η_{sub} thus provides a straightforward indicator on "how biased the resilience evaluation is if simply using the mean value of performance function".

With a log-Gamma $Q(t)$ in Eq. (30), for $t \in [0, \delta_1]$, it follows that,

$$\begin{aligned} \mu(Q(t+t_{\text{a}})) &= \psi_{\widetilde{X}(t)}(-1) = (1+b)^{-\widetilde{a}(t)} \\ \mu(Q^2(t+t_{\text{a}})) &= \psi_{\widetilde{X}(t)}(-2) = (1+2b)^{-\widetilde{a}(t)} \end{aligned} \tag{42}$$

Thus,

$$\overline{R}_{e,\text{sub},\overline{Q}} = \exp\left[\frac{1}{t_{\text{ref}}}\int_{t_{\text{a}}}^{t_{\text{b}}}\ln\overline{Q}(t)dt\right] = \exp\left[-\frac{\ln(b+1)}{t_{\text{ref}}}\int_0^{\delta_1}\widetilde{a}(t)dt\right] \tag{43}$$

Based on the definition of η_{sub}, one has,

$$\eta_{\text{sub}} = \exp\left\{-\frac{1}{t_{\text{ref}}}\int_0^{\delta_1}\widetilde{a}(t)\left[\frac{b}{1+\left(1-\frac{t}{\delta_1}\right)\frac{b\delta_1}{t_{\text{ref}}}} - \ln(b+1)\right]dt\right\} \tag{44}$$

For a special case where $\overline{Q}(t)$ degrades from 1 at time t_{a} to q_0 at time t_{b} with a linear $\widetilde{a}(t)$ with time, it follows that,

$$\overline{R}_{e,\text{sub},\overline{Q}} = q_0^{\frac{\delta_1}{2t_{\text{ref}}}}, \quad \eta_{\text{sub}} = q_0^{\mathcal{F}\left(b,\frac{\delta_1}{t_{\text{ref}}}\right)-\frac{\delta_1}{2t_{\text{ref}}}} \tag{45}$$

where

$$\mathcal{F}\left(b, \frac{\delta_1}{t_{\text{ref}}}\right) = \frac{\left(1 + \frac{t_{\text{ref}}}{b\delta_1}\right)\ln(1 + \frac{b\delta_1}{t_{\text{ref}}}) - 1}{\ln(b+1)} \tag{46}$$

Note that $\mathcal{F}\left(b, \frac{\delta_1}{t_{\text{ref}}}\right)$ is a monotonically increasing function of b. If b is an imprecise parameter and $b \in [b_{\text{lb}}, b_{\text{ub}}]$, then

$$q_0^{\mathcal{F}\left(b_{\text{ub}}, \frac{\delta_1}{t_{\text{ref}}}\right) - \frac{\delta_1}{2t_{\text{ref}}}} \leq \eta_{\text{sub}} \leq q_0^{\mathcal{F}\left(b_{\text{lb}}, \frac{\delta_1}{t_{\text{ref}}}\right) - \frac{\delta_1}{2t_{\text{ref}}}} \tag{47}$$

yielding the lower and upper bounds of η_{sub}. Otherwise, if the information on b_{lb} and b_{ub} is unknown, the bounds of η_{sub} are given as follows,

$$q_0^{1 - \frac{\delta_1}{2t_{\text{ref}}}} \leq \eta_{\text{sub}} \leq 1 \tag{48}$$

by noting that,

$$\lim_{b \to 0} \mathcal{F}\left(b, \frac{\delta_1}{t_{\text{ref}}}\right) = \frac{\delta_1}{2t_{\text{ref}}}, \quad \lim_{b \to \infty} \mathcal{F}\left(b, \frac{\delta_1}{t_{\text{ref}}}\right) = 1 \tag{49}$$

Eq. (48) shows that, if one substitutes the mean value of performance function into Eq. (33), the resilience would be overestimated since $\eta_{\text{sub}} \leq 1$.

Illustratively, Fig. 2(a) plots sampled trajectories and the mean value of $Q(t)$ with $\delta_1 = 5$ and $q_0 = 0.8$ (assuming $t_{\text{a}} = 0$). The coefficient of variation (COV) of $Q(\delta_1)$ equals 0.2, with which the value of b can be uniquely determined according to Eq. (42). The generation of a sample process $Q(t)$ is realized through first sampling a sequence of increments, $\Delta_1, \Delta_2, \ldots, \Delta_n$, and then computing $X(t)$ at discrete time instants $\delta_1/n, 2\delta_1/n, \ldots, \delta_1$. In Fig. 2(a), the simulated mean value of $Q(t)$ converges to 0.8 when $t = \delta_1$, which equals q_0 as expected.

Corresponding to the configuration in Fig. 2(a) but with an unknown value of b (or equivalently, unknown COV of $Q(\delta_1)$), the lower and upper bounds of η_{sub} are obtained according to Eq. (48) as 0.846 and 1, respectively with $t_{\text{ref}} = 10$. The value of η_{sub} as a function of b is computed by Eq. (44) and plotted in Fig. 2(b), which is found to vary within the bounds given by Eq. (48). Further, the accuracy of Eq. (44) has been verified in Fig. 2(b) via comparison between the analytical and simulation-based results.

In Fig. 2(b), the graph of η_{sub} as a function of b and its bounds associated with $q_0 = 0.4$ (i.e., more severe deterioration of performance function) are also presented with $t_{\text{ref}} = 10$. With a smaller value of q_0, the lower bound of η_{sub} becomes smaller (0.503 for $q_0 = 0.4$).

Lognormal process-based performance function

In this section, the use of lognormal stochastic process for the time-variation of performance function is discussed. For a time interval $[t_\mathrm{c}, t_\mathrm{d}] = [t_\mathrm{c}, t_\mathrm{c} + \delta_2]$, the performance function $Q(t)$ is modeled as follows: $Q(t) = \overline{Q}(t) \cdot E(t)$, in which $\overline{Q}(t) = \mu(Q(t))$, and $E(t)$ is a lognormal process with a mean value of 1, a standard deviation of σ_E, and a correlation coefficient of $\rho_E(t_2 - t_1)$ for $E(t_1)$ and $E(t_2)$, $t_\mathrm{c} \le t_1, t_2 \le t_\mathrm{d}$ (assume that $\rho_E(t_2 - t_1) \ge 0$). Note that the use of a lognormal process-based model does not require the monotonicity of $Q(t)$.

Applying the resilience model in Eq. (33), one has,

$$\begin{aligned}\overline{R}_{e,\mathrm{sub}} &= \mu\left(\exp\left[\frac{1}{t_\mathrm{ref}}\int_{t_\mathrm{c}}^{t_\mathrm{d}} \ln \overline{Q}(t)dt\right] \cdot \exp\left[\frac{1}{t_\mathrm{ref}}\int_{t_\mathrm{c}}^{t_\mathrm{d}} \ln E(t)dt\right]\right) \\ &= \underbrace{\exp\left[\frac{1}{t_\mathrm{ref}}\int_{t_\mathrm{c}}^{t_\mathrm{d}} \ln \overline{Q}(t)dt\right]}_{\overline{R}_{e,\mathrm{sub},\overline{Q}}} \cdot \mu\left(\exp(\Lambda)\right)\end{aligned} \tag{50}$$

where Λ is defined as follows,

$$\Lambda := \frac{1}{t_\mathrm{ref}}\int_{t_\mathrm{c}}^{t_\mathrm{d}} \ln E(t)dt = \frac{\delta_2}{t_\mathrm{ref}} \cdot \frac{1}{\delta_2}\int_{t_\mathrm{c}}^{t_\mathrm{d}} \alpha(t)dt \tag{51}$$

in which $\alpha(t) \equiv \ln E(t)$ is a stationary Gaussian process with a mean value of $\mu_\alpha = -0.5\ln(1 + \sigma_E^2)$, a standard deviation of $\sigma_\alpha = \sqrt{\ln(\sigma_E^2 + 1)}$, and an autocorrelation function of

$$\mathcal{R}_\alpha(t_2 - t_1) = \mu_\alpha^2 + \sigma_\alpha^2 \rho_\alpha(t_2 - t_1) = \mu_\alpha^2 + \sigma_\alpha^2 \frac{\ln[1 + \sigma_E^2 \cdot \rho_E(t_2 - t_1)]}{\ln(1 + \sigma_E^2)} \tag{52}$$

It has been shown in Eq. (50) that the bias factor η_sub equals $\mu\left(\exp(\Lambda)\right)$.

Assume that Eq. (51) contains a Riemann integral. Subdividing the time interval $[t_\mathrm{c}, t_\mathrm{d}]$ into n identical sections ($n \to \infty$), let $\Delta t = \delta_2/n$, $t_i = t_\mathrm{c} + i\delta_2/n$, and $\alpha_i = \alpha(t_i)$ for $i = 1, 2, \ldots n$. With this, it follows that,

$$\Lambda = \frac{\delta_2}{t_\mathrm{ref}} \cdot \lim_{n\to\infty} \frac{1}{\delta_2} \sum_{i=1}^{n} \alpha_i \Delta t \tag{53}$$

Based on Eq. (53), the first and second order moments of Λ are obtained as follows,

$$\mu(\Lambda) = \frac{\delta_2}{t_{\text{ref}}} \cdot \lim_{n\to\infty} \frac{1}{\delta_2} \sum_{i=1}^{n} \mu(\alpha_i)\Delta t = \frac{\delta_2}{t_{\text{ref}}} \cdot \mu_\alpha \tag{54}$$

and

$$\begin{aligned}\mu(\Lambda^2) &= \left(\frac{\delta_2}{t_{\text{ref}}}\right)^2 \cdot \lim_{n\to\infty} \left(\frac{\Delta t}{\delta_2}\right)^2 \mu\left(\sum_{i=1}^{n}\alpha_i\right)^2 = \left(\frac{\delta_2}{t_{\text{ref}}}\right)^2 \cdot \lim_{n\to\infty} \frac{1}{n^2} \sum_{i=1}^{n}\sum_{j=1}^{n} \mu(\alpha_i\alpha_j) \\ &= \left(\frac{\delta_2}{t_{\text{ref}}}\right)^2 \cdot \int_0^{\delta_2} \mathcal{R}_\alpha(\tau) f_{\Delta^*}(\tau)d\tau\end{aligned} \tag{55}$$

in which $f_{\Delta^*}(\tau)$ is the PDF of Δ^* (the difference of two time instants that are randomly and uniformly selected from $[t_\text{c}, t_\text{d}]$), $f_{\Delta^*}(\tau) = 2(1-\tau/\delta_2)/\delta_2$ for $\tau \in [0, \delta_2]$. With this, Eq. (55) is rewritten as follows,

$$\begin{aligned}\mu(\Lambda^2) &= \left(\frac{\delta_2}{t_{\text{ref}}}\right)^2 \cdot \frac{2}{\delta_2} \int_0^{\delta_2} [\mu_\alpha^2 + \rho_\alpha(\tau)\cdot\sigma_\alpha^2] \cdot \left(1 - \frac{\tau}{\delta_2}\right) d\tau \\ &= \left(\frac{\delta_2}{t_{\text{ref}}}\right)^2 \cdot \left[\mu_\alpha^2 + \frac{2\sigma_\alpha^2}{\delta_2} \int_0^{\delta_2} \frac{\ln[1+\sigma_E^2\cdot\rho_E(\tau)]}{\ln(1+\sigma_E^2)} \cdot \left(1 - \frac{\tau}{\delta_2}\right) d\tau\right]\end{aligned} \tag{56}$$

with which the variance of Λ is evaluated according to,

$$\begin{aligned}\sigma^2(\Lambda) = \mu(\Lambda^2) - \mu^2(\Lambda) &= \left(\frac{\delta_2}{t_{\text{ref}}}\right)^2 \cdot \frac{2\ln(\sigma_E^2+1)}{\delta_2} \int_0^{\delta_2} \frac{\ln[1+\sigma_E^2\cdot\rho_E(\tau)]}{\ln(1+\sigma_E^2)} \cdot \left(1 - \frac{\tau}{\delta_2}\right) d\tau \\ &= \frac{2\delta_2}{t_{\text{ref}}^2} \int_0^{\delta_2} \ln[1+\sigma_E^2\cdot\rho_E(\tau)] \cdot \left(1 - \frac{\tau}{\delta_2}\right) d\tau\end{aligned} \tag{57}$$

Recall that Λ is a normal variable according to Eq. (53). Thus,

$$\begin{aligned}\eta_{\text{sub}} &= \mu\left(\exp(\Lambda)\right) = \exp\left[\mu(\Lambda) + 0.5\sigma^2(\Lambda)\right] \\ &= \exp\left[-\frac{\delta_2}{2t_{\text{ref}}} \cdot \ln(1+\sigma_E^2) + \frac{\delta_2}{t_{\text{ref}}^2} \int_0^{\delta_2} \ln[1+\sigma_E^2\cdot\rho_E(\tau)] \cdot \left(1 - \frac{\tau}{\delta_2}\right) d\tau\right]\end{aligned} \tag{58}$$

Substituting Eq. (58) into (50), the explicit form of resilience is derived.

In Eq. (58), if $\rho_E(\tau)$ is an imprecise function of τ satisfying $\rho_E(\tau) \in [\rho_{E,\text{lb}}, \rho_{E,\text{ub}}]$, then

$$\eta_{\text{sub}} \in \left[\left(1+\sigma_E^2\right)^{-\frac{\delta_2}{2t_{\text{ref}}}} \cdot \left(1+\rho_{E,\text{lb}}\sigma_E^2\right)^{\frac{\delta_2^2}{2t_{\text{ref}}^2}}, \left(1+\sigma_E^2\right)^{-\frac{\delta_2}{2t_{\text{ref}}}} \cdot \left(1+\rho_{E,\text{ub}}\sigma_E^2\right)^{\frac{\delta_2^2}{2t_{\text{ref}}^2}}\right] \tag{59}$$

yielding the lower and upper bounds for η_{sub}. However, if the information on $\rho_{E,\text{lb}}$ and $\rho_{E,\text{ub}}$ is unknown, since $\rho_E(\tau)$ varies within $[0, 1]$, the interval for η_{sub} is as follows,

$$\eta_{\text{sub}} \in \left[\left(1 + \sigma_E^2\right)^{-\frac{\delta_2}{2t_{\text{ref}}}}, \left(1 + \sigma_E^2\right)^{\frac{\delta_2^2}{2t_{\text{ref}}^2} - \frac{\delta_2}{2t_{\text{ref}}}} \right] \tag{60}$$

The accuracy and applicability of the bounds for η_{sub} in Eq. (60) are examined through a numerical example. Assume that the autocorrelation function of $E(t)$ takes a form of

$$\mathcal{R}_E(\tau) = (1 + \sigma_E^2)^{\exp(-k\tau^2)}, \quad k \geq 0 \tag{61}$$

where k is a non-negative parameter. Fig. 3(a) shows the dependence of $\mathcal{R}_E(\tau)$ on τ with some specific values of k and σ_E. With this, the autocorrelation function of $\alpha(t)$ is

$$\mathcal{R}_\alpha(\tau) = \mu_\alpha^2 + \sigma_\alpha^2 \exp(-k\tau^2) \tag{62}$$

Denote $\widetilde{\alpha}(t) \equiv \alpha(t) - \mu_\alpha$, with which $\mathcal{R}_{\widetilde{\alpha}}(\tau) = \sigma_\alpha^2 \exp(-k\tau^2)$, and the power spectral density (PSD) function of $\widetilde{\alpha}(t)$, $\mathbb{S}_{\widetilde{\alpha}}(\omega)$ is,

$$\mathbb{S}_{\widetilde{\alpha}}(\omega) = \frac{1}{\pi} \int_0^\infty \sigma_\alpha^2 \exp(-k\tau^2) \cos(\omega\tau) d\tau = \sigma_\alpha^2 \cdot \frac{1}{2\sqrt{k\pi}} \exp\left(-\frac{\omega^2}{4k}\right) \tag{63}$$

Assume that $\delta_2 = 5$ and $t_{\text{ref}} = 10$. The lower and upper bounds of η_{sub} are dependent on σ_E according to Eq. (60), and are plotted in Fig. 3(b) for $\sigma_E = 1$ and 2, respectively. These bounds define an interval for η_{sub} in Eq. (58) as a function of k (note that k affects the correlation structure of $E(t)$). Further, the accuracy of Eq. (58) is verified through employing the MC method to generate simulation-based η_{sub}. To this end, by noting that $\widetilde{\alpha}(t)$ is a zero-mean Gaussian process, the following approach can be used to generate a sample process for $\widetilde{\alpha}(t)$ (Shinozuka 1971),

$$\widetilde{\alpha}(t) = \sigma_\alpha \sqrt{\frac{2}{N}} \cdot \sum_{j=1}^{N} \cos\left(\Omega_j t + U_j\right) \tag{64}$$

where N is a sufficiently large integer, Ω_j is a real random variable with a PDF of $f_\Omega(\omega) = \mathbb{S}_{\widetilde{\alpha}}(\omega)/\sigma_\alpha^2$, and U_j is a random variable that is uniformly distributed in $[0, 2\pi]$. The agreement between the analytical and simulated results in Fig. 3(b) demonstrates the accuracy of Eq. (58).

Bounds of time-dependent imprecise resilience

In the section, the bounding method for time-dependent imprecise resilience, $\overline{R}_e(0, t_l)$, will be discussed, which is also applicable to handle the imprecise resilience problem over $[t_0, t_h]$ in Eq. (4).

Two types of stochastic processes have been discussed above (log-Gamma and lognormal) to model the time-variation of performance functions. For a planning horizon of $[0, t_l]$, $Q(t)$ may display inconsistent monotonicity characteristics within different time intervals (subsets of $[0, t_l]$), as previously addressed in Eq. (29). Motivated by this observation, the reference period $[0, t_l]$ is subdivided into N_D sub-intervals, namely $\mathcal{D}_1, \mathcal{D}_2, \ldots, \mathcal{D}_{N_D}$, that satisfy $\bigcup_{i=1}^{N_D} \mathcal{D}_i = [0, t_l]$ and $\mathcal{D}_i \bigcap \mathcal{D}_j = \emptyset, \forall i \neq j$ simultaneously. Let $\overline{R}_{e,\mathrm{sub},i}$ be the resilience associated with $\mathcal{D}_i$. Assume that the performance function over $\mathcal{D}_i$ is statistically independent of that over $\mathcal{D}_j$ for $\forall i \neq j$. Based on Eq. (5), it follows that,

$$\begin{aligned}\overline{R}_e(0, t_l) &= \mu\left\{\exp\left[\frac{1}{t_l}\int_{\bigcup_{i=1}^{N_D}\mathcal{D}_i} \ln[Q(t)]dt\right]\right\} = \mu\left\{\exp\left[\frac{1}{t_l}\sum_{i=1}^{N_D}\int_{\mathcal{D}_i} \ln[Q(t)]dt\right]\right\} \\ &= \mu\left\{\prod_{i=1}^{N_D}\exp\left[\frac{1}{t_l}\int_{\mathcal{D}_i} \ln[Q(t)]dt\right]\right\} = \prod_{i=1}^{N_D}\mu\left\{\exp\left[\frac{1}{t_l}\int_{\mathcal{D}_i} \ln[Q(t)]dt\right]\right\} \\ &= \prod_{i=1}^{N_D}\overline{R}_{e,\mathrm{sub},i}\end{aligned} \tag{65}$$

Let $\overline{R}_{e,\mathrm{lb},i}$ and $\overline{R}_{e,\mathrm{ub},i}$ be the lower and upper bounds of $\overline{R}_{e,\mathrm{sub},i}$, respectively. According to Eq. (65), it follows that,

$$\prod_{i=1}^{N_D}\overline{R}_{e,\mathrm{lb},i} \leq \overline{R}_e(0, t_l) \leq \prod_{i=1}^{N_D}\overline{R}_{e,\mathrm{ub},i} \tag{66}$$

which gives the lower and upper bounds for $\overline{R}_e(0, t_l)$.

Let $\eta(0, t_l)$ denote the bias factor for $\overline{R}_e(0, t_l)$, which is defined, similar to η_{sub}, as the ratio of $\overline{R}_e(0, t_l)$ to $\overline{R}_{e,\overline{Q}}(0, t_l)$ (the time-dependent resilience based on the mean performance function), and is calculated as follows,

$$\begin{aligned}\eta(0, t_l) &= \frac{\overline{R}_e(0, t_l)}{\overline{R}_{e,\overline{Q}}(0, t_l)} = \frac{\mu\left\{\exp\left[\frac{1}{t_l}\int_0^{t_l} \ln[Q(t)]dt\right]\right\}}{\exp\left[\frac{1}{t_l}\int_0^{t_l} \ln[\overline{Q}(t)]dt\right]} \\ &= \frac{\prod_{i=1}^{N_D}\overline{R}_{e,\mathrm{sub},i}}{\prod_{i=1}^{N_D}\overline{R}_{e,\overline{Q},i}} = \prod_{i=1}^{N_D}\eta_{\mathrm{sub},i}\end{aligned} \tag{67}$$

in which $\overline{R}_{e,\overline{Q},i}$ is the resilience based on the mean value of performance function associated with $\mathcal{D}_i$, and $\eta_{\mathrm{sub},i}$ is the bias factor for $\overline{R}_{e,\mathrm{sub},i}$, $i = 1, 2, \ldots N_D$. Let $\eta_{\mathrm{lb},i}$ and $\eta_{\mathrm{ub},i}$ be the lower and upper bounds of $\eta_{\mathrm{sub},i}$, respectively. Based on Eq. (67), the bounds for $\eta(0, t_l)$ is given as follows,

$$\prod_{i=1}^{N_D} \eta_{\mathrm{lb},i} \leq \eta(0, t_l) \leq \prod_{i=1}^{N_D} \eta_{\mathrm{ub},i} \tag{68}$$

Note that the lower and upper bounds for η_{sub} presented in Eqs. (47), (48) and Eqs. (59), (60) have considered the imprecise information on one parameter associated with the stochastic performance function (b and ρ_E, respectively), which are indeed an application of Eq. (16). The other parameters involved in the sub resilience problems (see Eqs. (41) and (50)) could also be imprecise in a probabilistic sense. In such a case, the resilience bounding techniques (e.g., the interval MC method, and LP-based method) can be employed to determine the bounds of the imprecise resilience. For example, consider the resilience problem of a reinforced concrete (RC) structure in a marine environment subjected to chloride ingress. The performance of the structure is deemed to be 100% from the initial time ($t = 0$) until crack initiation ($t = T_i$). Then the performance function deteriorates gradually until the appearance of crack on the concrete surface ($t = T_i + T_{ci}$). With this, the sub resilience problem over $[T_i, T_i + T_{ci}]$ can be evaluated by Eq. (33), where $t_{\mathrm{a}} = T_i$ and $t_{\mathrm{b}} = T_i + T_{ci}$. Note also that both T_i and $T_i + T_{ci}$ are affected by many factors of the RC structure, such as the concrete thickness, apparent diffusion coefficient, cross-section area of steel bars, corrosion rate, and others (Vidal et al. 2004; El Maaddawy and Soudki 2007; Li and Ye 2018; Wang 2021a). If one or several of these factors are incompletely informed (e.g., only the low order moments are available), the bounding techniques for imprecise resilience apply. Another example is presented in the next section, where the time-dependent resilience of a strip foundation in a changing climate is examined. The imprecise information on the sea level rise (SLR), which is a key influencing factor for the foundation resilience, is quantified using the LP-based method.

EXAMPLE

In this section, an example is presented to demonstrate the applicability of the proposed bounding techniques for imprecise resilience. Consider the serviceability of a strip foundation located in a coastal area, as previously studied in Wang et al. (2023). The load bearing capacity of the foundation, R_{ult}, is as follows,

$$R_{\mathrm{ult}} = cN_c + \gamma D_{\mathrm{f}} N_q + 0.5\gamma B_{\mathrm{f}} N_\gamma \tag{69}$$

in which c is the cohesion of soil, γ is the unit weight of soil, D_{f} and B_{f} are the depth and width of the foundation, respectively (as illustrated in Fig. 4(a)), and N_c, N_q, N_γ are three functions of the soil internal friction angle ϕ expressed as follows,

$$N_q = \tan^2\left(\frac{\pi}{4} + \frac{\phi}{2}\right)\exp(\pi \tan\phi) \tag{70}$$

$$N_c = (N_q - 1)\cot\phi \tag{71}$$

$$N_\gamma = 2(N_q + 1)\tan\phi \tag{72}$$

Note that Eq. (69) holds if the groundwater table is below the foundation bottom with a distance of at least B_f. However, due to the potential impact of groundwater table rise as a result of SLR in a changing climate, this condition could be violated. In such a case, one would need to modify Eq. (69). If the groundwater table is above the foundation bottom at a distance of x_a (see Case 1 in Fig. 4(a)), then R_ult is expressed as follows,

$$R_\mathrm{ult} = cN_c + [\gamma(D_\mathrm{f} - x_a) + x_a(\gamma_\mathrm{sa} - \gamma_w)]N_q + 0.5(\gamma_\mathrm{sa} - \gamma_w)B_\mathrm{f}N_\gamma \tag{73}$$

in which γ_sa is the saturated unit weight of soil, and γ_w is the unit weight of water (9.81 kN/m³). On the other hand, if the groundwater table is below the foundation bottom at a distance of x_b (Case 2 in Fig. 4(a)), then Eq. (69) is modified as,

$$R_\mathrm{ult} = cN_c + \gamma D_\mathrm{f}N_q + 0.5\left[(\gamma_\mathrm{sa} - \gamma_w) + \frac{x_b}{B_\mathrm{f}}(\gamma - \gamma_\mathrm{sa} + \gamma_w)\right]B_\mathrm{f}N_\gamma \tag{74}$$

The statistics of γ, ϕ and γ_sa used in this example are presented in Table 1. The foundation has a width of 0.9 m and a depth of 0.6 m, and the initial groundwater table is 1.8 m below the ground level. Assume that the soil cohesion is negligible (so that $c = 0$), and that the groundwater table rise is equal to SLR. A reference period of 80 years will be considered, within which the sea level may rise by 0.5 m – 1.4 m, as projected in National Research Council (2012b).

The performance function of the foundation is dependent on the time-variant load bearing capacity R_ult. The reduction of R_ult is initiated when the groundwater table arrives at a distance of B_f below the foundation bottom. Before this time point, the performance function is full (see "Stage 1" in Fig. 4(b)). Subsequently, the gradual deterioration of $Q(t)$ as a result of the decreasing R_ult is referred to as "Stage 2", until R_ult reaches a predefined threshold (0.9 times the initial state in this example). This corresponds to a mean value of q_0 for the performance function. The conduction of repair actions is then triggered to restore the load bearing capacity to the initial state (e.g., via groundwater drawdown), leading to the recovery the performance function (Stage 3). The duration of recovery process follows a normal distribution with a mean value of 2 years and a COV of 0.2. The time-variation of $Q(t)$ is modeled by a log-Gamma process for Stage 2, and a lognormal process for Stage 3. Note that for a reference period of $[0, t_l]$, the sequence of Stages 1–2–3 may occur for multiple times.

Fig. 5 shows sampled trajectories of $Q(t)$ over a reference period of 80 years with $q_0 = 0.7$, $b_{\text{ub}} \to 0$ and $\sigma_E \to 0$ (recall that b_{ub} is the upper bound of the scale parameter of $-\ln Q(t)$ in Eq. (30), and σ_E is the standard deviation of $E(t)$ in Eq. (50)). Four representative values of SLR are considered in Fig. 5, representing different scenarios of climate change. For each case, the performance function is full (100%) from the initial time (or the completion of the previous recovery process) until the reduction initiation of R_{ult}, followed by the stage of gradual deterioration (Stage 2) in parallel with the decreasing load bearing capacity, and Stage 3 of performance function recovery.

Fig. 6 plots the lower and upper bounds of time-dependent imprecise resilience for reference periods up to 80 years according to Eq. (66). The imprecision is associated with the gradual deterioration and recovery processes of the performance function (see Stages 2 and 3 in Fig. 4), with $q_0 = 0.7$, $b_{\text{ub}} = 10$ and $\sigma_E = 0.5$. Four cases of SLR are considered, with an increase of 0.5 m, 0.8 m, 1.1 m and 1.4 m, respectively, over 80 years, representing different scenarios of climate change. For comparison purpose, the resilience evaluated with $\overline{Q}(t)$, $\overline{R}_{e,\overline{Q}}(0, t_l)$, is also presented in Fig. 6. The upper bound of imprecise resilience is below $\overline{R}_{e,\overline{Q}}(0, t_l)$, because the upper bound of η_{sub} is less than 1 for both log-Gamma and lognormal processes. This indicates that, the resilience would be overestimated (non-conservative) if simply using the mean value of performance function in the resilience assessment. Further, a more severe scenario of SLR leads to smaller values of resilience bounds but wider intervals (greater difference between lower and upper bounds). For example, the lower bound equals 0.892, 0.854, 0.834 and 0.808 respectively for a reference period of 80 years in Figs. 6(a–d), indicating the amplified possibility of low resilience in a more severe climate change pattern.

The impact of q_0 (i.e., the mean value of performance function immediately before repair measures) on the bounds of $\eta(0, t_l)$ (the bias factor for time-dependent resilience) is shown in Table 2, where $\sigma_E = 0.5$, $b_{\text{ub}} = \infty$ and SLR = 1.4 m over 80 years. With a fixed t_l, the lower bound of $\eta(0, t_l)$ becomes larger with a greater value of q_0. This is because, according to Eqs. (47) and (60), the lower bound of the bias factor is

$q_0^{1-\frac{\delta_1}{2t_{\text{ref}}}} \cdot \left(1+\sigma_E^2\right)^{-\frac{\delta_2}{2t_{\text{ref}}}}$ conditional on δ_1, δ_2 for one deterioration-recovery cycle of performance function, which is an increasing function of q_0. On the other hand, the upper bound of the bias factor in Table 2 is $\left(1+\sigma_E^2\right)^{\frac{\delta_2^2}{2t_{\text{ref}}^2}-\frac{\delta_2}{2t_{\text{ref}}}}$, which is independent of q_0. The observation from Table 2 is consistent with that from Fig. 2(b), where the lower bound of η_{sub} associated with $q_0 = 0.4$ is smaller than that associated with $q_0 = 0.8$.

The dependence of the bounds of time-dependent imprecise resilience on b_{ub} is examined in Fig. 7(a), where $q_0 = 0.7$, $\sigma_E = 0.5$, and SLR = 1.4 m over 80 years. While the upper bound of resilience is independent of b_{ub}, the lower bound of resilience becomes smaller with a larger value of b_{ub}. For example, for a reference period of 80 years, the lower bound of resilience is 0.887 if $b_{\text{ub}} = 1$, which becomes 0.710 if $b_{\text{ub}} = 100$, and 0.554 with $b_{\text{ub}} = \infty$. This is because $\mathcal{F}$ in Eq. (46) is a monotonically increasing function of b, and thus $q_0^{\mathcal{F}}$ in Eq. (47) decreases with b_{ub}.

The impact of σ_E on the resilience bounds is presented in Fig. 7(b) with $q_0 = 0.7$, $b_{\text{ub}} = 10$, and SLR = 1.4 m over 80 years. A greater value of σ_E means larger uncertainty associated with the recovery process, and thus reduced bounds for resilience (both lower and upper). For example, the lower bound equals 0.811 and 0.789 for a reference period of 80 years corresponding to $\sigma_E = 0.1$ and 2, respectively. This observation is consistent with Eq. (60), where the exponents of the two bounds, $-\delta_2/(2t_{\text{ref}})$ and $\delta_2^2/(2t_{\text{ref}}^2) - \delta_2/(2t_{\text{ref}})$, are both negative.

Next, the role of imprecise information on SLR in time-dependent resilience is investigated. Assume that the SLR over the next 80 years, which is treated as an imprecise random variable, has a mean value of 1m and a COV of 0.3, and is bounded between 0.5 m and 1.4 m. However, the distribution type of SLR is unknown. In such a case, one can use the LP-based method (see Eqs. (25) and (26)) to find the lower and upper bounds of resilience. In terms of the uncertainty associated with the gradual deterioration and recovery of $Q(t)$, the following two cases are considered: (1) $b_{\text{ub}} \to 0$ and $\sigma_E \to 0$, and (2) $b_{\text{ub}} = 10$ and $\sigma_E = 0.5$. For the two cases, the bounds of time-dependent resilience over a reference period of 40, 60 and 80 years are presented in Table 3 with $q_0 = 0.7$. The (lower or upper) bound associated with case (1) is greater than that associated with case (2), because additional uncertainty arising from the deterioration and recovery processes of $Q(t)$ has been included in case (2). This observation suggests the importance of properly incorporating all the uncertainty sources in resilience assessment.

CONCLUDING REMARKS

In this paper, a novel method for the assessment of imprecise resilience has been proposed, which handles resilience problems in the presence of non-probabilistic information on the performance function. The lower and upper bounds of imprecise resilience are produced through the proposed bounding techniques, which have benefitted from those for imprecise reliability. In particular, since the resilience is measured based on the integration of performance function over time, two types of stochastic processes are discussed to model the time-variation of performance function, namely log-Gamma and lognormal. The following conclusions can be drawn from this paper.

1. Existing bounding techniques for imprecise releasability, including interval MC method and LP-based method, can be extended to handle imprecise resilience problems, motivated by a unified framework for reliability and resilience assessment from a mathematical perspective.
2. The resilience be measured through subdividing the reference period of interest into multiple time intervals, and integrating the resiliences associated with these sub-intervals. Under independence assumption on the performance functions over these intervals, the (lower or upper) bound of imprecise resilience equals the multiplication of the resilience bounds associated with each sub-interval.
3. In the presence of uncertain and imprecise performance function $Q(t)$, the resilience would be over-estimated if using the mean value of $Q(t)$ in the resilience assessment, since the upper bound of the bias factor is less than 1.
4. The importance of considering climate change in resilience evaluation is demonstrated through examining the time-dependent resilience of a strip foundation. For a reference period of 80 years in Fig. 6, the resilience interval is $[0.892, 0.964]$ with SLR = 0.5 m over 80 years, and becomes $[0.808, 0.912]$ if SLR = 1.4 m over 80 years.

In future works, it is an interesting topic to investigate the sensitivity of resilience bounds to the correlation between the performance functions over different sub-intervals.

DATA AVAILABILITY STATEMENT

All data, models, or code that support the findings of this study are available from the corresponding author upon reasonable request.

ACKNOWLEDGEMENTS

The research described in this paper was supported by the Career Development Fellowship for Cao Wang from the University of Wollongong. This support is gratefully acknowledged.

REFERENCES

Alvarez, D. A. and Hurtado, J. E. (2014). "An efficient method for the estimation of structural reliability intervals with random sets, dependence modeling and uncertain inputs." *Computers & Structures*, 142, 54–63.

Attoh-Okine, N. O., Cooper, A. T., and Mensah, S. A. (2009). "Formulation of resilience index of urban infrastructure using belief functions." *IEEE Systems Journal*, 3(2), 147–153.

Augustin, T., Coolen, F. P., De Cooman, G., and Troffaes, M. C. (2014). *Introduction to imprecise probabilities*. John Wiley & Sons.

Beer, M., Ferson, S., and Kreinovich, V. (2013). "Imprecise probabilities in engineering analyses." *Mechanical Systems and Signal Processing*, 37(1–2), 4–29.

Bocchini, P., Frangopol, D. M., Ummenhofer, T., and Zinke, T. (2014). "Resilience and sustainability of civil infrastructure: Toward a unified approach." *Journal of Infrastructure Systems*, 20(2), 04014004.

Bruneau, M., Chang, S. E., Eguchi, R. T., Lee, G. C., O'Rourke, T. D., Reinhorn, A. M., Shinozuka, M., Tierney, K., Wallace, W. A., and Von Winterfeldt, D. (2003). "A framework to quantitatively assess and enhance the seismic resilience of communities." *Earthquake Spectra*, 19(4), 733–752.

Cimellaro, G. P., Reinhorn, A. M., and Bruneau, M. (2010). "Framework for analytical quantification of disaster resilience." *Engineering Structures*, 32(11), 3639–3649.

Coolen, F. (2004). "On the use of imprecise probabilities in reliability." *Quality and Reliability Engineering International*, 20(3), 193–202.

Dang, C., Wei, P., Faes, M. G., and Beer, M. (2022). "Bayesian probabilistic propagation of hybrid uncertainties: Estimation of response expectation function, its variable importance and bounds." *Computers & Structures*, 270, 106860.

Dubois, D. and Prade, H. (1989). "Fuzzy sets, probability and measurement." *European Journal of Operational Research*, 40(2), 135–154.

El Maaddawy, T. and Soudki, K. (2007). "A model for prediction of time from corrosion initiation to corrosion cracking." *Cement and Concrete Composites*, 29(3), 168–175.

Ellingwood, B. R. (2005). "Risk-informed condition assessment of civil infrastructure: state of practice and research issues." *Structure and Infrastructure Engineering*, 1(1), 7–18.

Faes, M. G., Broggi, M., Chen, G., Phoon, K.-K., and Beer, M. (2022). "Distribution-free p-box processes based on translation theory: Definition and simulation." *Probabilistic Engineering Mechanics*, 69, 103287.

Faes, M. G., Daub, M., Marelli, S., Patelli, E., and Beer, M. (2021a). "Engineering analysis with probability boxes: A review on computational methods." *Structural Safety*, 93, 102092.

Faes, M. G., Valdebenito, M. A., Moens, D., and Beer, M. (2020). "Bounding the first excursion probability of linear structures subjected to imprecise stochastic loading." *Computers & Structures*, 239, 106320.

Faes, M. G., Valdebenito, M. A., Moens, D., and Beer, M. (2021b). "Operator norm theory as an efficient tool to propagate hybrid uncertainties and calculate imprecise probabilities." *Mechanical Systems and Signal Processing*, 152, 107482.

Faes, M. G., Valdebenito, M. A., Yuan, X., Wei, P., and Beer, M. (2021c). "Augmented reliability analysis for estimating imprecise first excursion probabilities in stochastic linear dynamics." *Advances in Engineering Software*, 155, 102993.

Ferson, S., Kreinovich, V., Ginzburg, L., Myers, D. S., and Sentz, K. (2003). "Constructing probability boxes and Dempster-Shafer structures." *Report No. SAND2002–4015*, Sandia National Laboratories, https://doi.org/10.2172/809606.

Kahle, W., Mercier, S., and Paroissin, C. (2016). *Gamma Processes*. John Wiley & Sons, Chapter 2, 49–148.

Kahraman, C., Öztayşi, B., and Çevik Onar, S. (2016). "A comprehensive literature review of 50 years of fuzzy set theory." *International Journal of Computational Intelligence Systems*, 9(sup1), 3–24.

Li, Q. and Ye, X. (2018). "Surface deterioration analysis for probabilistic durability design of RC structures in marine environment." *Structural Safety*, 75, 13–23.

Limbourg, P. and De Rocquigny, E. (2010). "Uncertainty analysis using evidence theory–confronting level-1 and level-2 approaches with data availability and computational constraints." *Reliability Engineering & System Safety*, 95(5), 550–564.

Melchers, R. E. and Beck, A. T. (2018). *Structural reliability analysis and prediction*. John Wiley & Sons.

National Research Council (2012a). *Disaster resilience: A national imperative*. The National Academies Press, Washington DC.

National Research Council (2012b). *Sea-Level Rise for the Coasts of California, Oregon, and Washington: Past, Present, and Future*. The National Academies Press, Washington DC.

Oberguggenberger, M. and Fellin, W. (2008). "Reliability bounds through random sets: Non-parametric methods and geotechnical applications." *Computers & Structures*, 86(10), 1093–1101.

Penmetsa, R. C. and Grandhi, R. V. (2002). "Efficient estimation of structural reliability for problems with uncertain intervals." *Computers & Structures*, 80, 1103–1112.

Ross, S. M. (2014). *Introduction to probability models*. Academic Press.

Shinozuka, M. (1971). "Simulation of multivariate and multidimensional random processes." *The Journal of the Acoustical Society of America*, 49(1B), 357–368.

Utkin, L. V. and Coolen, F. P. (2007). *Imprecise reliability: an introductory overview*. Springer, 261–306.

Vidal, T., Castel, A., and François, R. (2004). "Analyzing crack width to predict corrosion in reinforced concrete." *Cement and Concrete Research*, 34(1), 165–174.

Walley, P. (2000). "Towards a unified theory of imprecise probability." *International Journal of Approximate Reasoning*, 24, 125–148.

Wang, C. (2021a). "Explicitly assessing the durability of RC structures considering spatial variability and correlation." *Infrastructures*, 6(11), 156.

Wang, C. (2021b). *Structural Reliability and Time-Dependent Reliability*. Springer Nature Switzerland AG.

Wang, C. (2023). "A generalized index for functionality-sensitive resilience quantification." *Resilient Cities and Structures*, 2(1), 68–75.

Wang, C. and Ayyub, B. M. (2022). "Time-dependent resilience of repairable structures subjected to nonstationary load and deterioration for analysis and design." *ASCE-ASME Journal of Risk and Uncertainty in Engineering Systems, Part A: Civil Engineering*, 8(3), 04022021.

Wang, C., Ayyub, B. M., and Kumari, W. G. P. (2023). "Resilience model for coastal-building foundations with time-variant soil strength due to water intrusion in a changing climate." *Rock and Soil Mechanics*, 44(1), 67–74.

Wang, C., Zhang, H., and Beer, M. (2018). "Computing tight bounds of structural reliability under imprecise probabilistic information." *Computers & Structures*, 208, 92–104.

Wei, P., Song, J., Bi, S., Broggi, M., Beer, M., Lu, Z., and Yue, Z. (2019). "Non-intrusive stochastic analysis with parameterized imprecise probability models: I. performance estimation." *Mechanical Systems and Signal Processing*, 124, 349–368.

Wu, D., Gao, W., Tin-Loi, F., and Pi, Y. (2016). "Probabilistic interval limit analysis for structures with hybrid uncertainty." *Engineering Structures*, 114, 195–208.

Wu, W.-Z., Leung, Y., and Zhang, W.-X. (2002). "Connections between rough set theory and Dempster-Shafer theory of evidence." *International Journal of General Systems*, 31(4), 405–430.

Zhang, H. (2012). “Interval importance sampling method for finite element-based structural reliability assessment under parameter uncertainties.” *Structural Safety*, 38, 1–10.

Zhang, H., Mullen, R. L., and Muhanna, R. L. (2010). “Interval Monte Carlo methods for structural reliability.” *Structural Safety*, 32(3), 183–190.

Zhang, J. and Shields, M. D. (2019). “Efficient monte carlo resampling for probability measure changes from Bayesian updating.” *Probabilistic Engineering Mechanics*, 55, 54–66.

592 TABLES

TABLE 1. Statistics of random variables associated with soil properties.

Variable	Mean	COV	Distribution type
Unit weight of soil γ	16 kN/m³	0.15	Lognormal
Soil friction angle ϕ	30°	0.10	Lognormal
Saturated unit weight of soil γ_{sa}	18 kN/m³	0.15	Lognormal

TABLE 2. Dependence on q_0 of the bounds of $\eta(0, t_l)$.

q_0	t_l = 40 years		t_l = 60 years		t_l = 80 years	
	Lower	Upper	Lower	Upper	Lower	Upper
0.6	0.713	0.9974	0.566	0.9969	0.491	0.9963
0.7	0.788	0.9974	0.668	0.9969	0.605	0.9963
0.8	0.860	0.9974	0.773	0.9969	0.728	0.9963
0.9	0.930	0.9974	0.883	0.9969	0.858	0.9963

TABLE 3. Role of imprecise information on SLR in resilience bounds.

Case	t_l = 40 years		t_l = 60 years		t_l = 80 years	
	Lower	Upper	Lower	Upper	Lower	Upper
(1)	0.957	0.967	0.936	0.944	0.921	0.934
(2)	0.903	0.966	0.860	0.942	0.834	0.932

LIST OF FIGURES

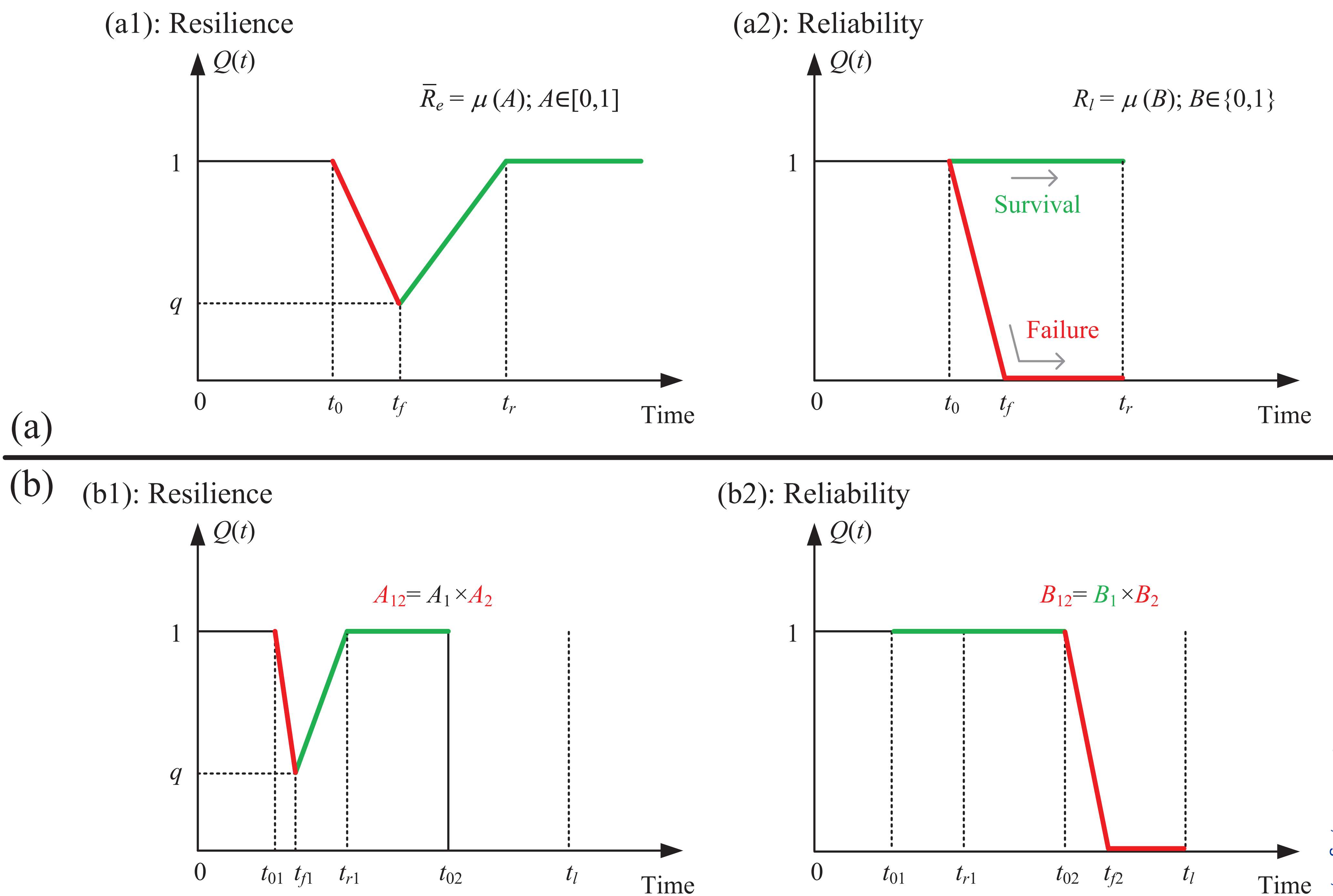
(a1): Resilience
Q(t)
$\bar{R}_e = \mu(A); A \in [0,1]$
1
q
0
t_0
t_f
t_r
Time
(a2): Reliability
Q(t)
$R_l = \mu(B); B \in \{0,1\}$
1
Survival
Failure
0
t_0
t_f
t_r
Time
(a)
(b)
(b1): Resilience
Q(t)
$A_{12} = A_1 \times A_2$
1
q
0
t_{01}
t_{f1}
t_{r1}
t_{02}
t_l
Time
(b2): Reliability
Q(t)
$B_{12} = B_1 \times B_2$
1
0
t_{01}
t_{r1}
t_{02}
t_{f2}
t_l
Time

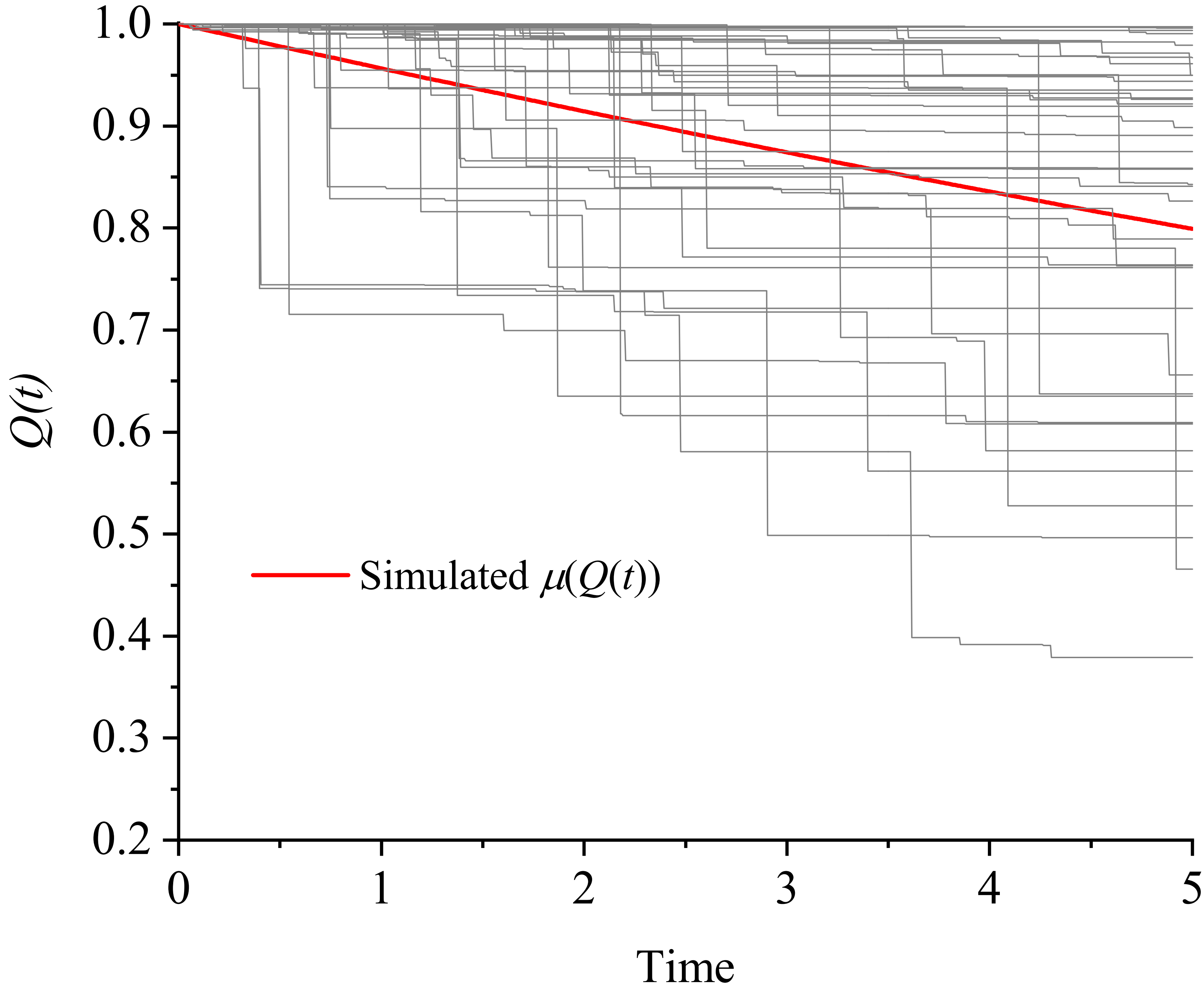
1.0
0.9
0.8
0.7
0.6
0.5
0.4
0.3
0.2
$Q(t)$
0
1
2
3
4
5
Time
Simulated $\mu(Q(t))$

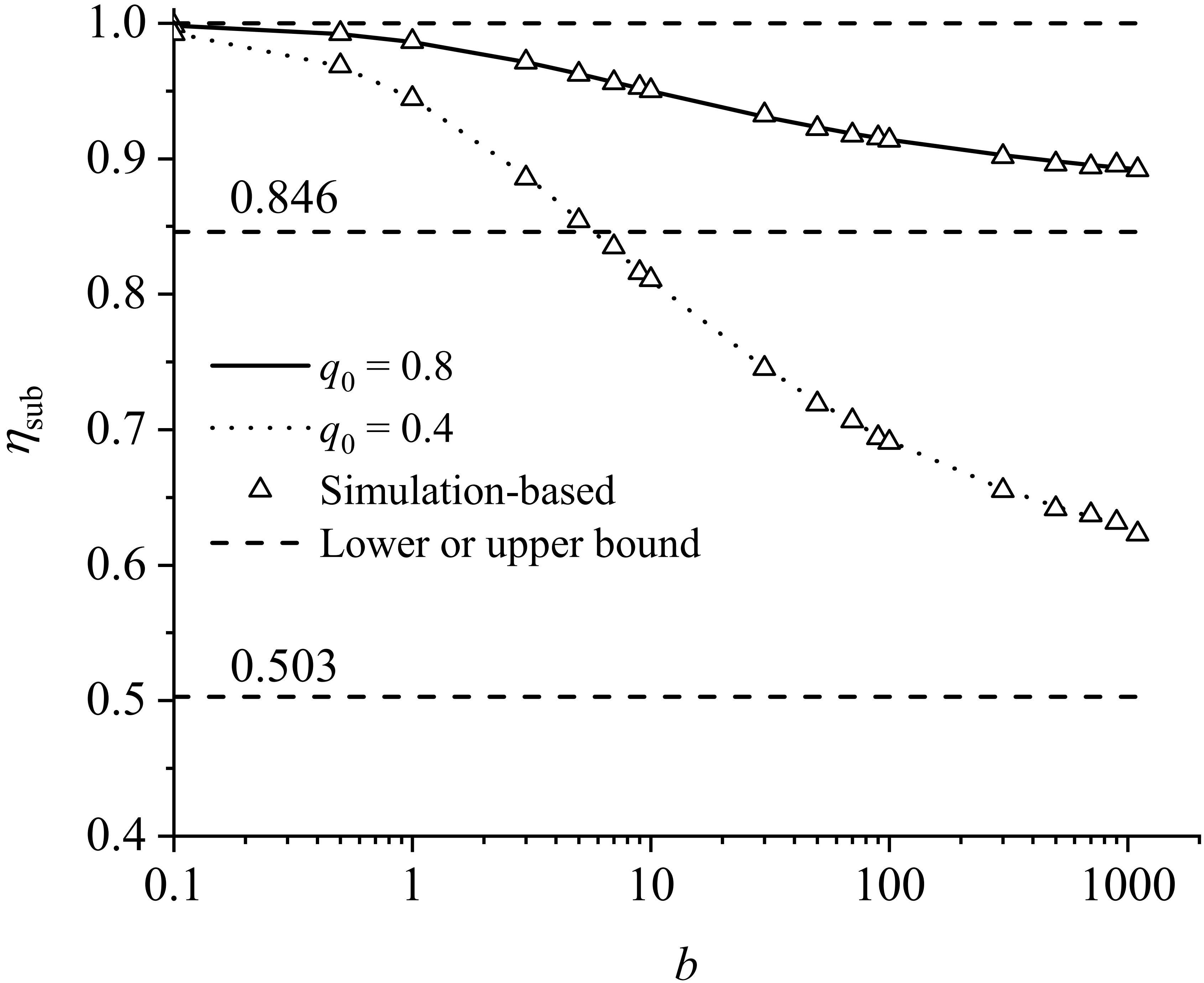
1.0
0.9
0.8
0.7
0.6
0.5
0.4
0.846
0.503
η_{sub}
$q_0 = 0.8$
$q_0 = 0.4$
Simulation-based
Lower or upper bound
0.1
1
10
100
1000
b

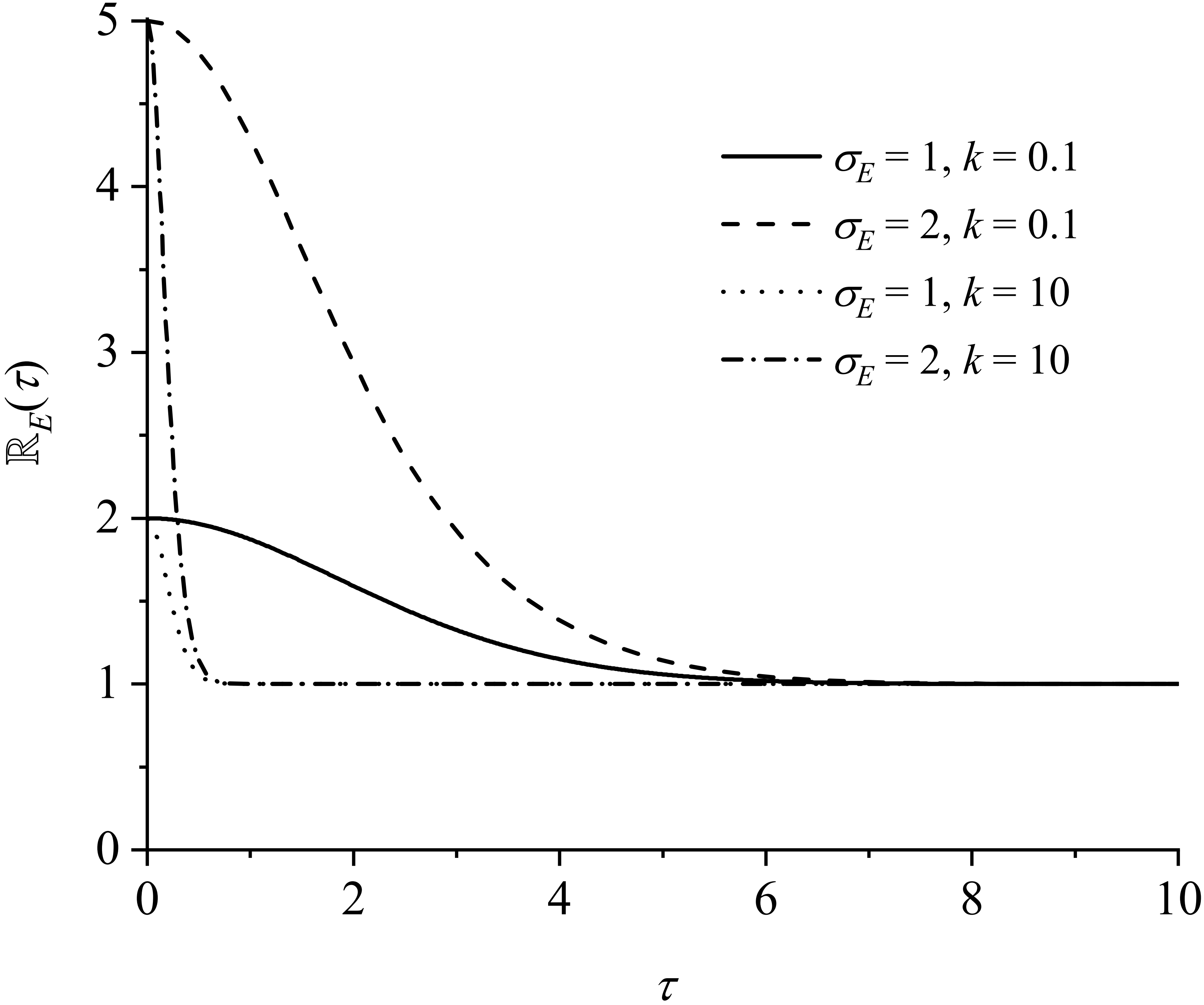

$\sigma_E = 1, k = 0.1$
$\sigma_E = 2, k = 0.1$
$\sigma_E = 1, k = 10$
$\sigma_E = 2, k = 10$
$\mathbb{R}_E(\tau)$
τ
0
1
2
3
4
5
0
2
4
6
8
10

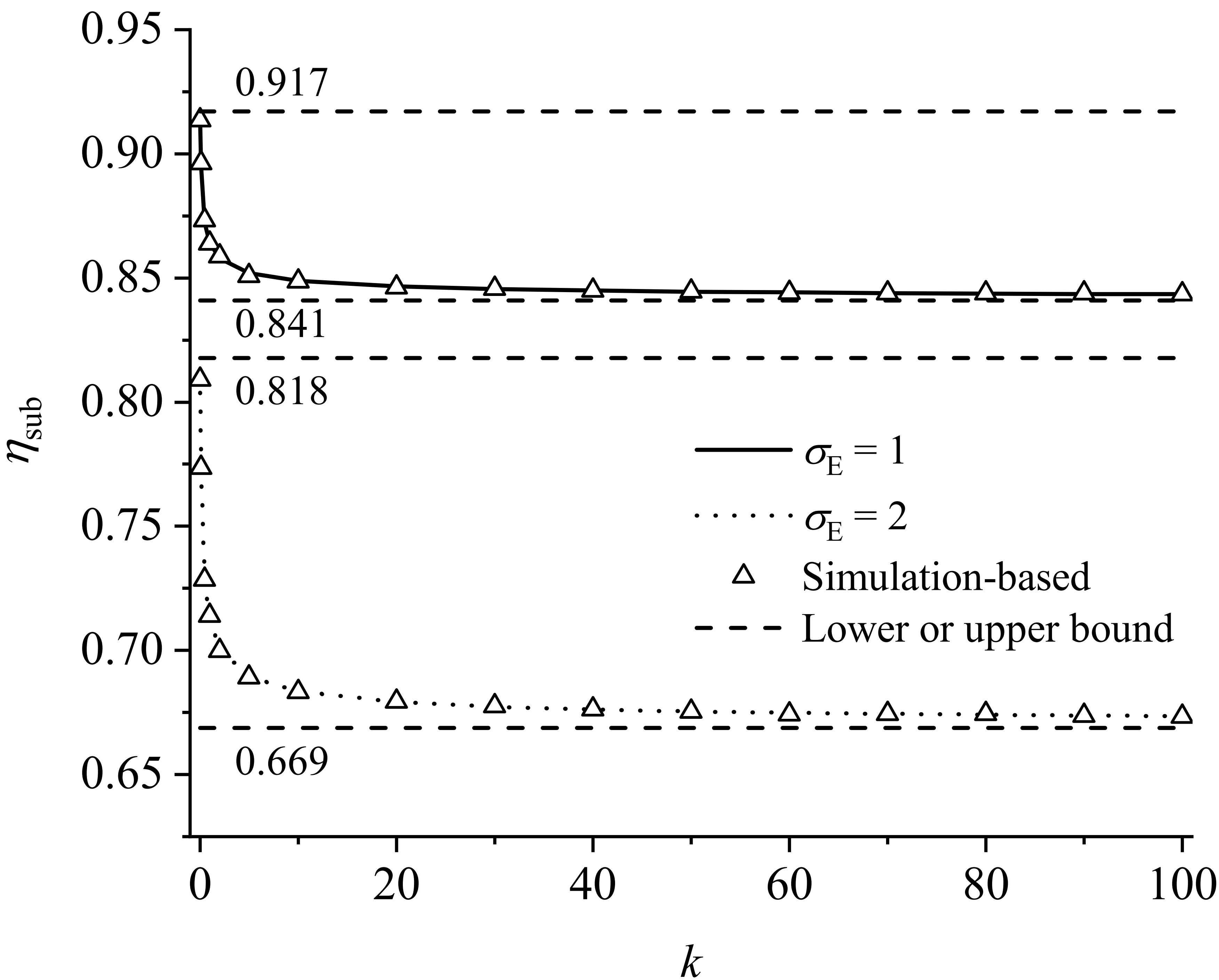

0.95
0.90
0.85
0.80
0.75
0.70
0.65
0.917
0.841
0.818
0.669
η_{sub}
$\sigma_E = 1$
$\sigma_E = 2$
Simulation-based
Lower or upper bound
0
20
40
60
80
100
k

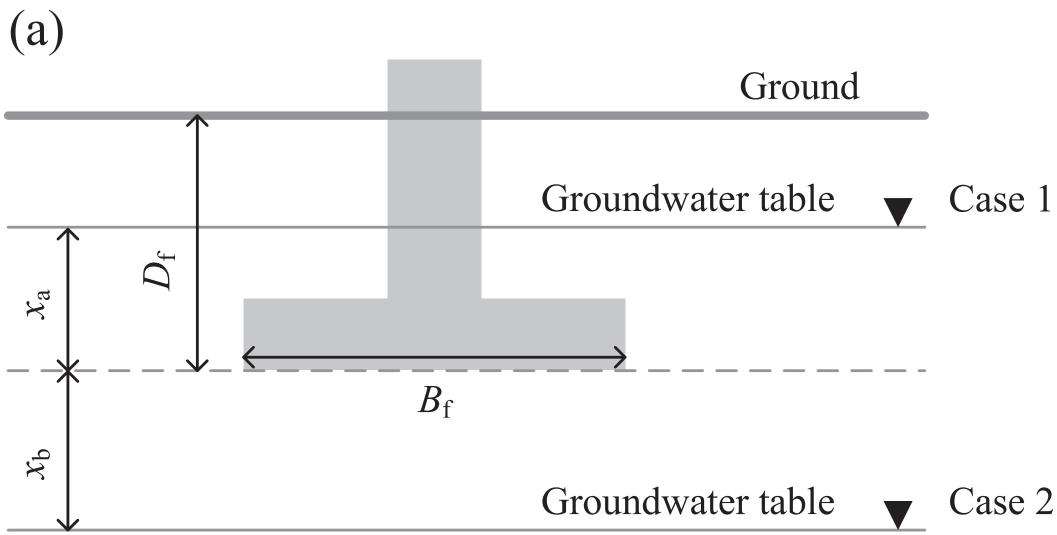
(a)
Ground
Groundwater table
Case 1
D_f
x_a
B_f
x_b
Groundwater table
Case 2

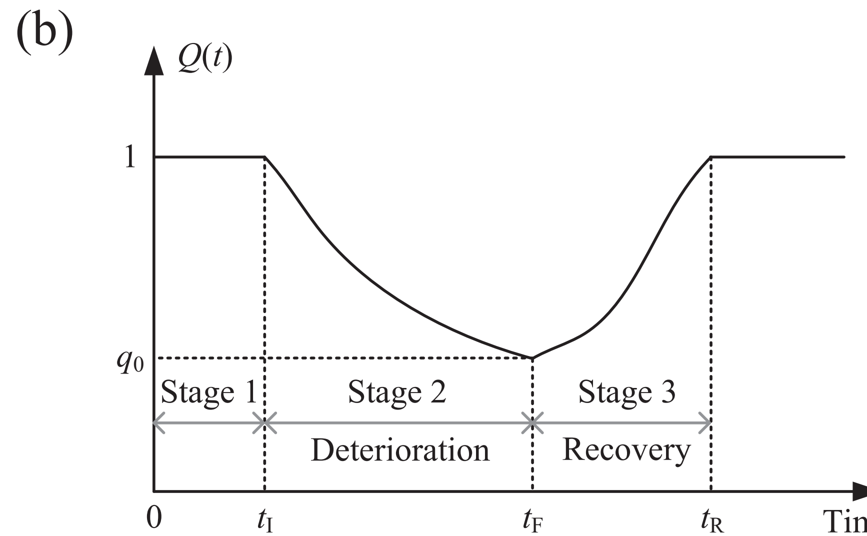
(b)
$Q(t)$
1
q_0
Stage 1
Stage 2
Stage 3
Deterioration
Recovery
0
t_I
t_F
t_R
Time

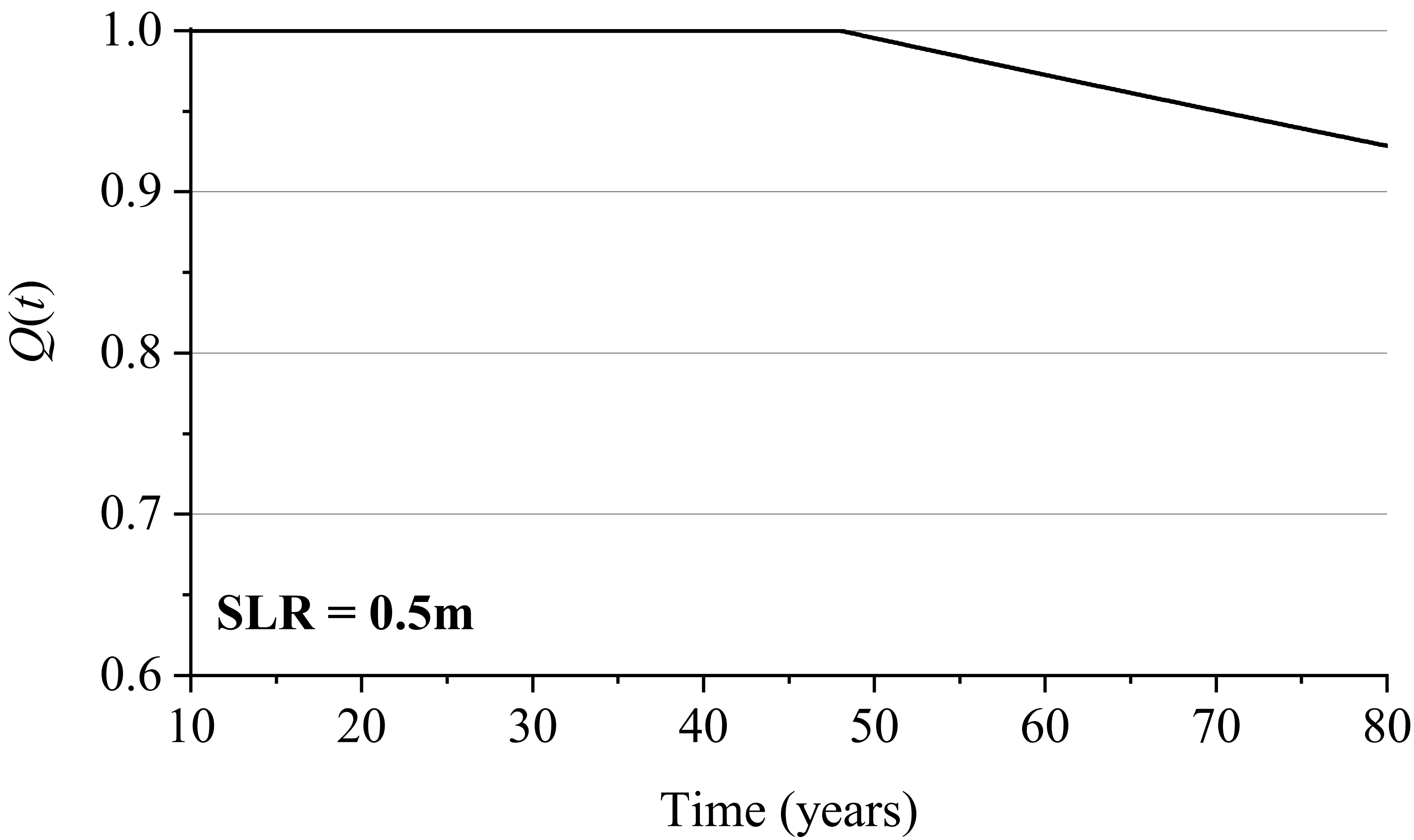
1.0
0.9
0.8
0.7
0.6
$Q(t)$
SLR = 0.5m
10
20
30
40
50
60
70
80
Time (years)

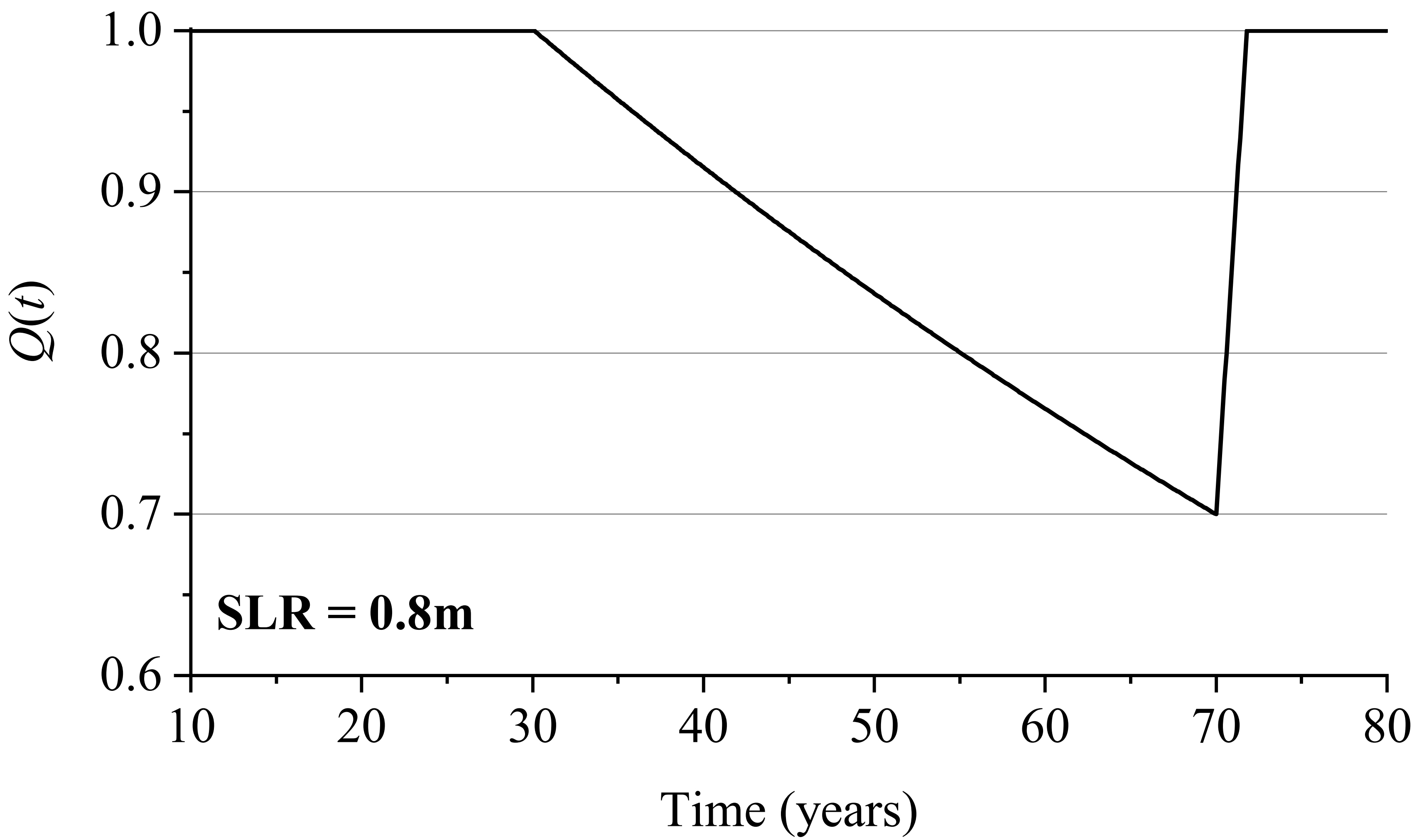
1.0
0.9
0.8
0.7
0.6
$Q(t)$
SLR = 0.8m
10
20
30
40
50
60
70
80
Time (years)

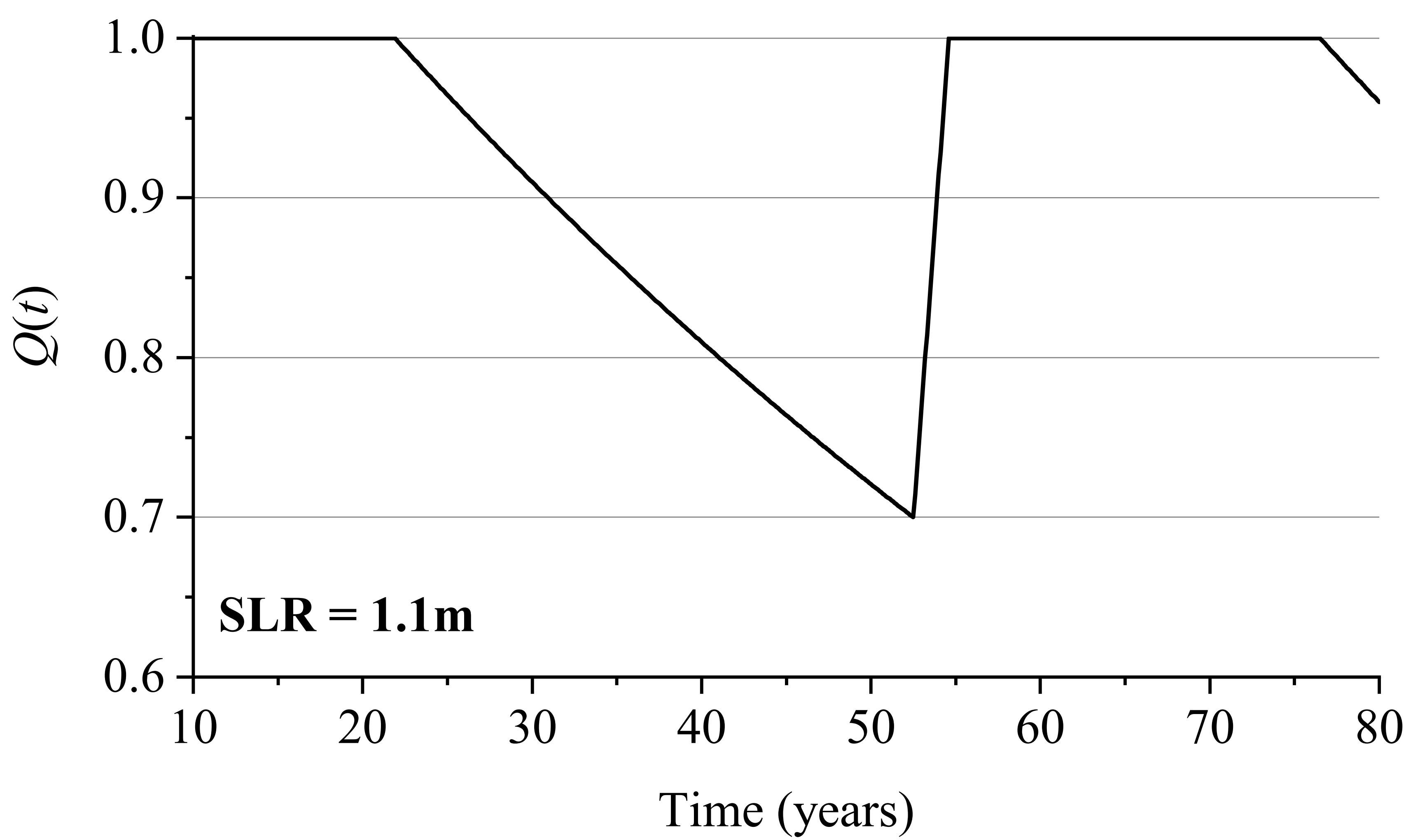

1.0
0.9
0.8
0.7
0.6
Q(t)
SLR = 1.1m
10
20
30
40
50
60
70
80
Time (years)

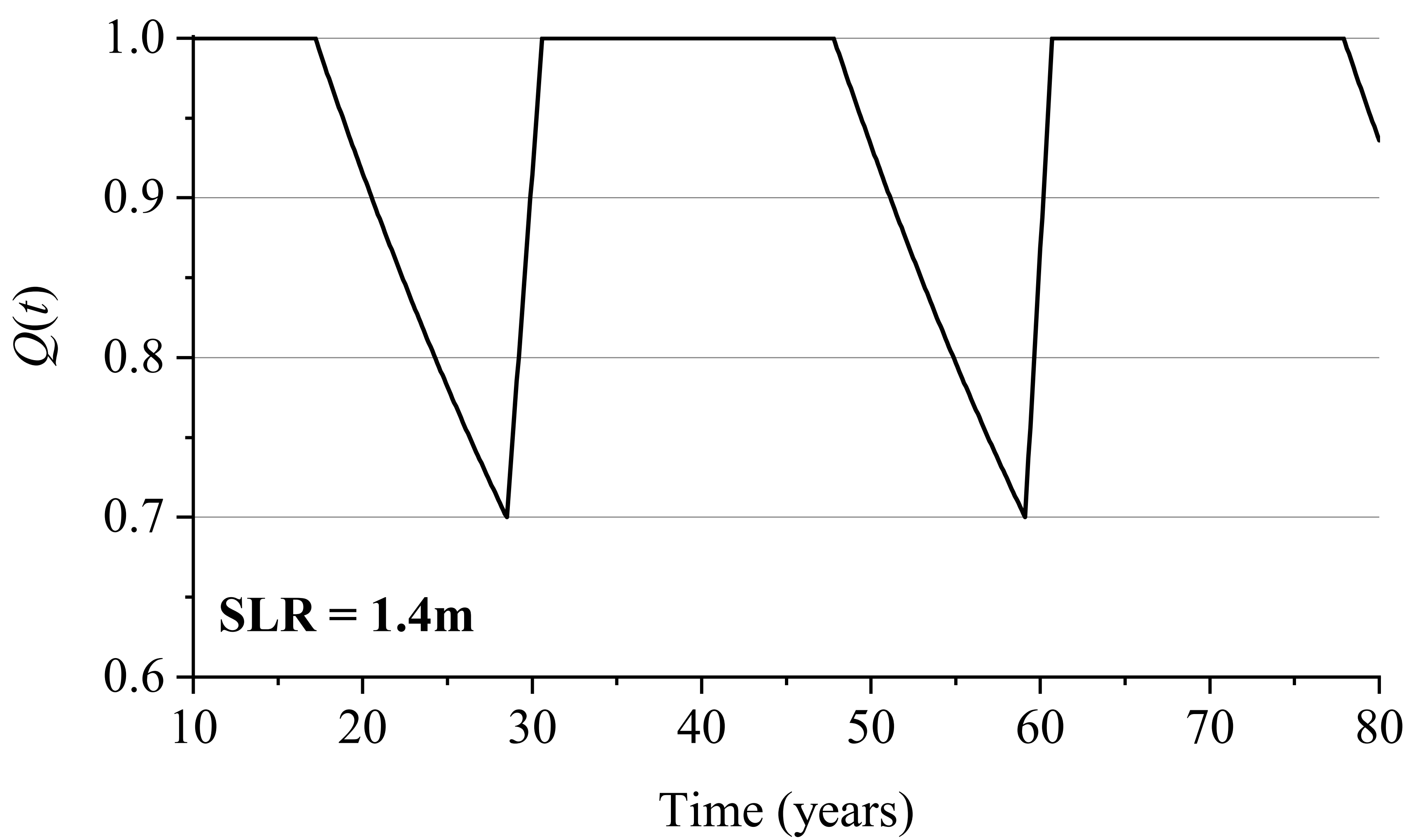

1.0
0.9
0.8
0.7
0.6
Q(t)
SLR = 1.4m
10
20
30
40
50
60
70
80
Time (years)

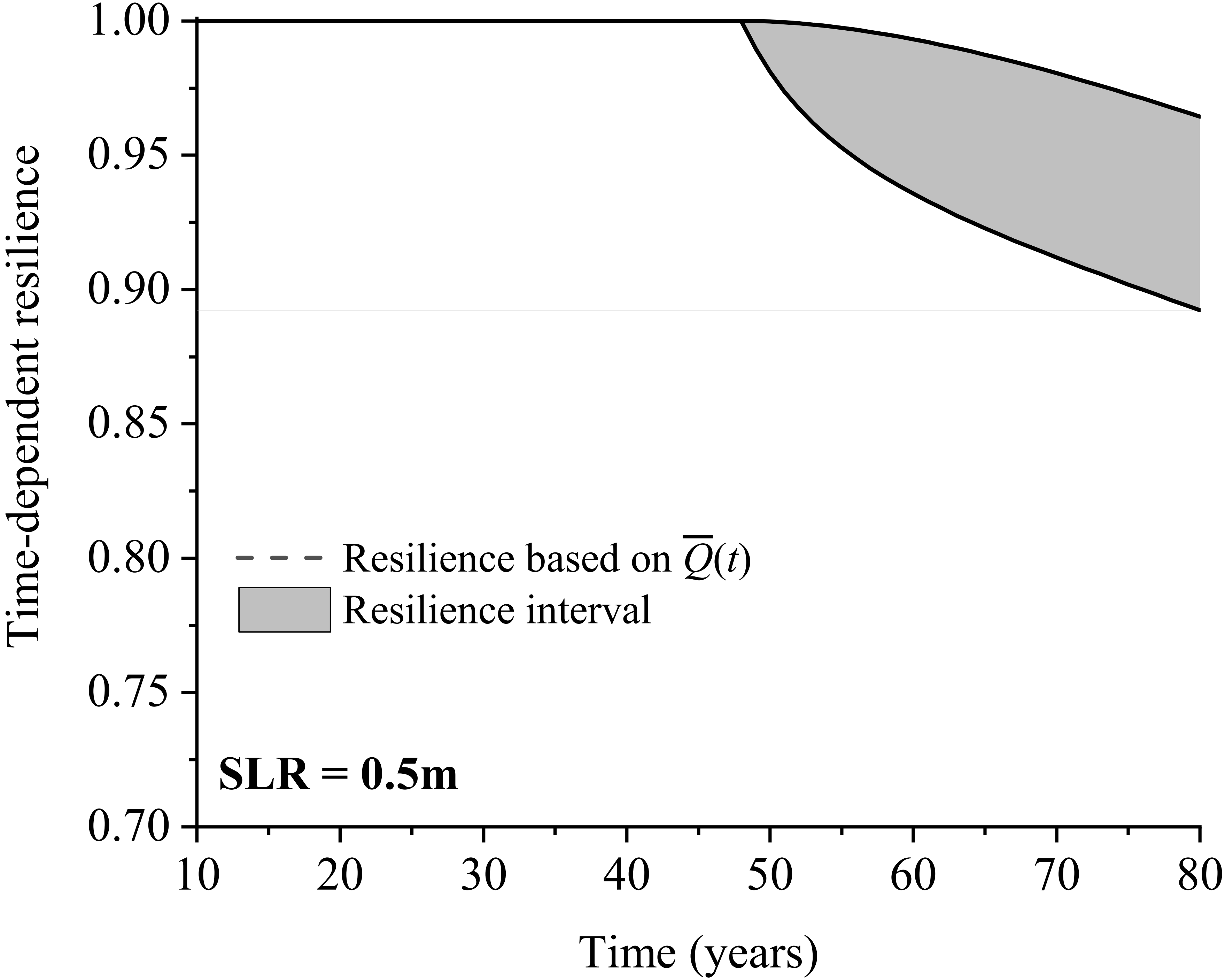
1.00
0.95
0.90
0.85
0.80
0.75
0.70
Time-dependent resilience
10
20
30
40
50
60
70
80
Time (years)
Resilience based on $\overline{Q}(t)$
Resilience interval
SLR = 0.5m

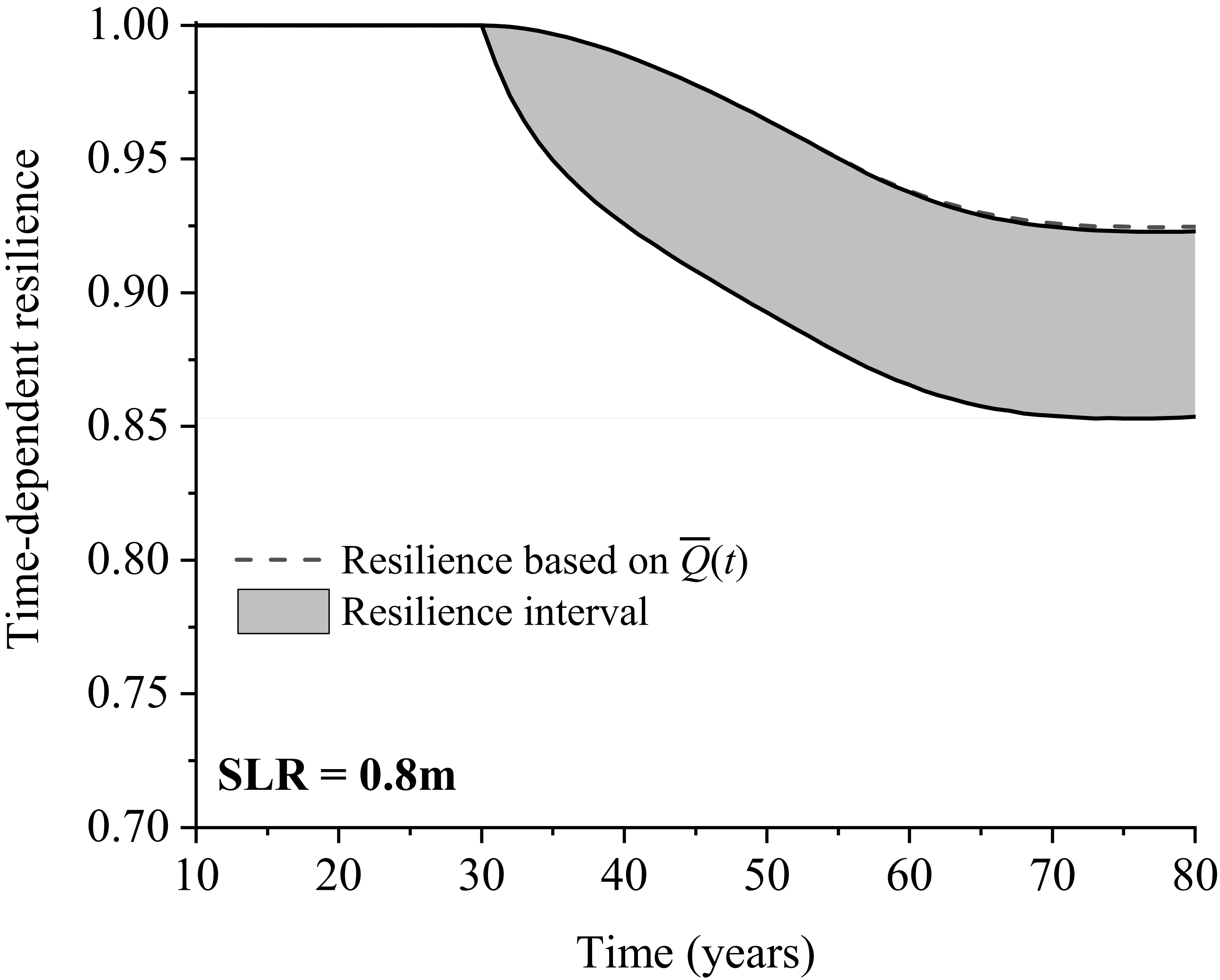
1.00
0.95
0.90
0.85
0.80
0.75
0.70
Time-dependent resilience
10
20
30
40
50
60
70
80
Time (years)
Resilience based on $\overline{Q}(t)$
Resilience interval
SLR = 0.8m

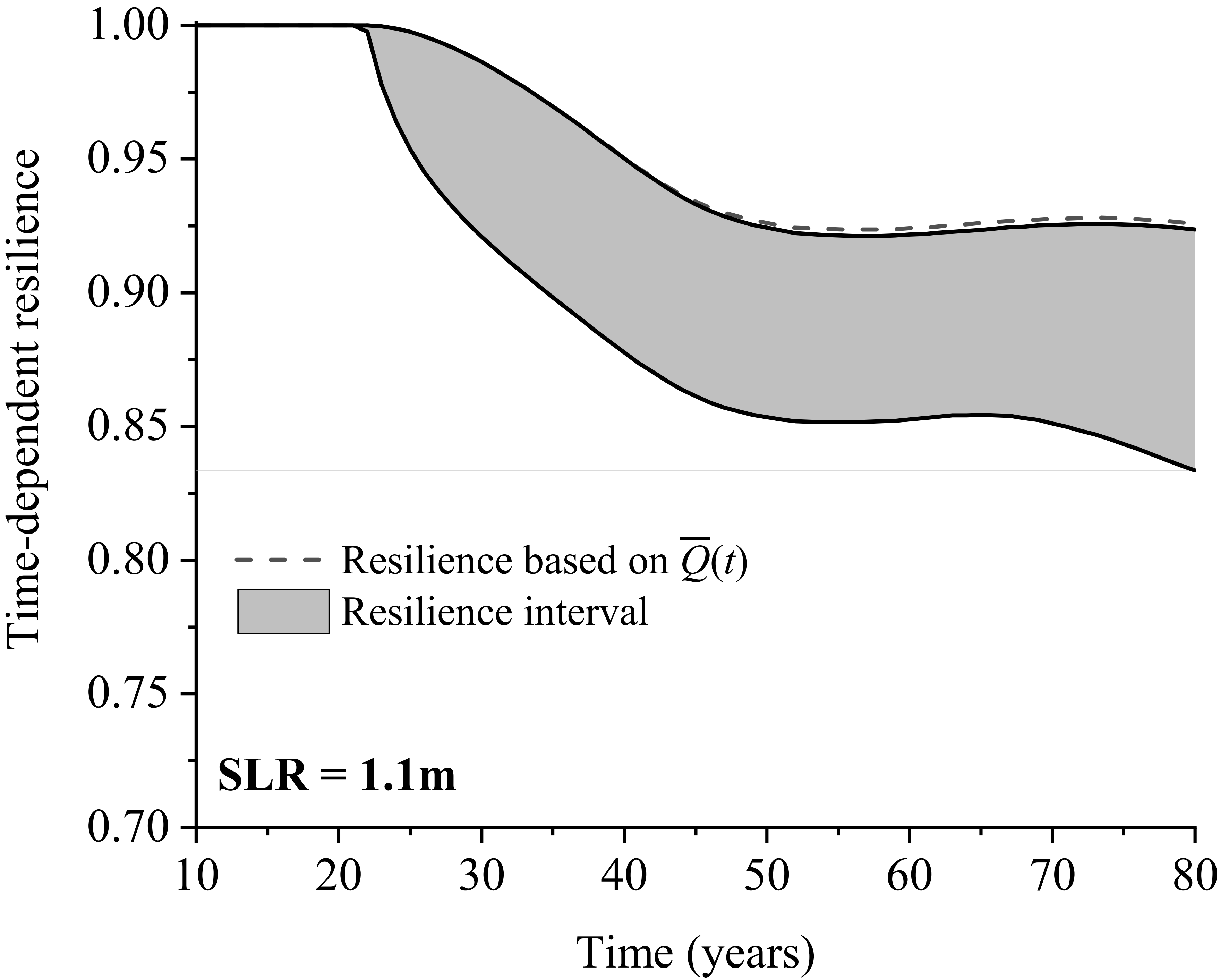

1.00
0.95
0.90
0.85
0.80
0.75
0.70
Time-dependent resilience
10
20
30
40
50
60
70
80
Time (years)
Resilience based on $\overline{Q}(t)$
Resilience interval
SLR = 1.1m

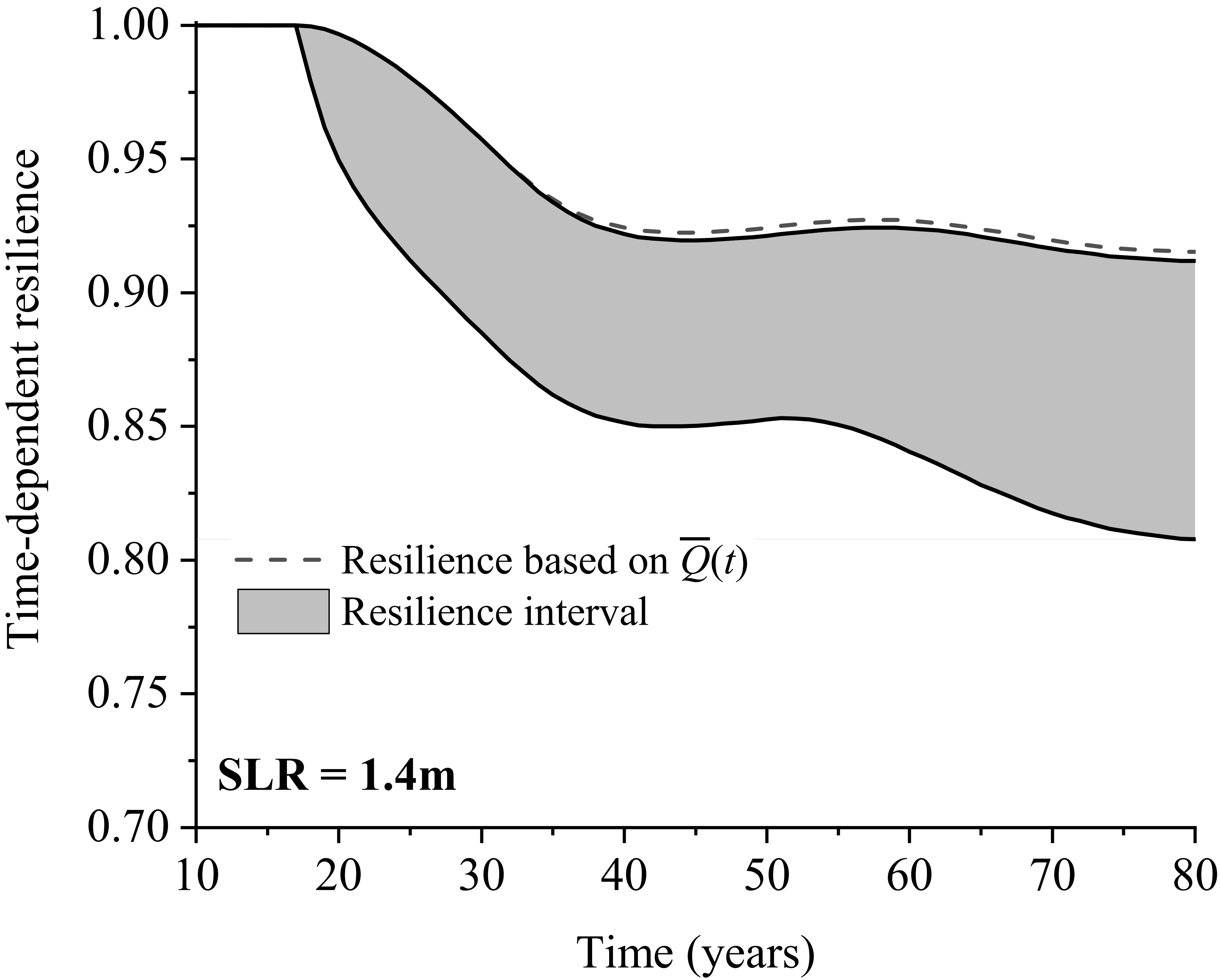
1.00
0.95
0.90
0.85
0.80
0.75
0.70
Time-dependent resilience
10
20
30
40
50
60
70
80
Time (years)
Resilience based on $\overline{Q}(t)$
Resilience interval
SLR = 1.4m

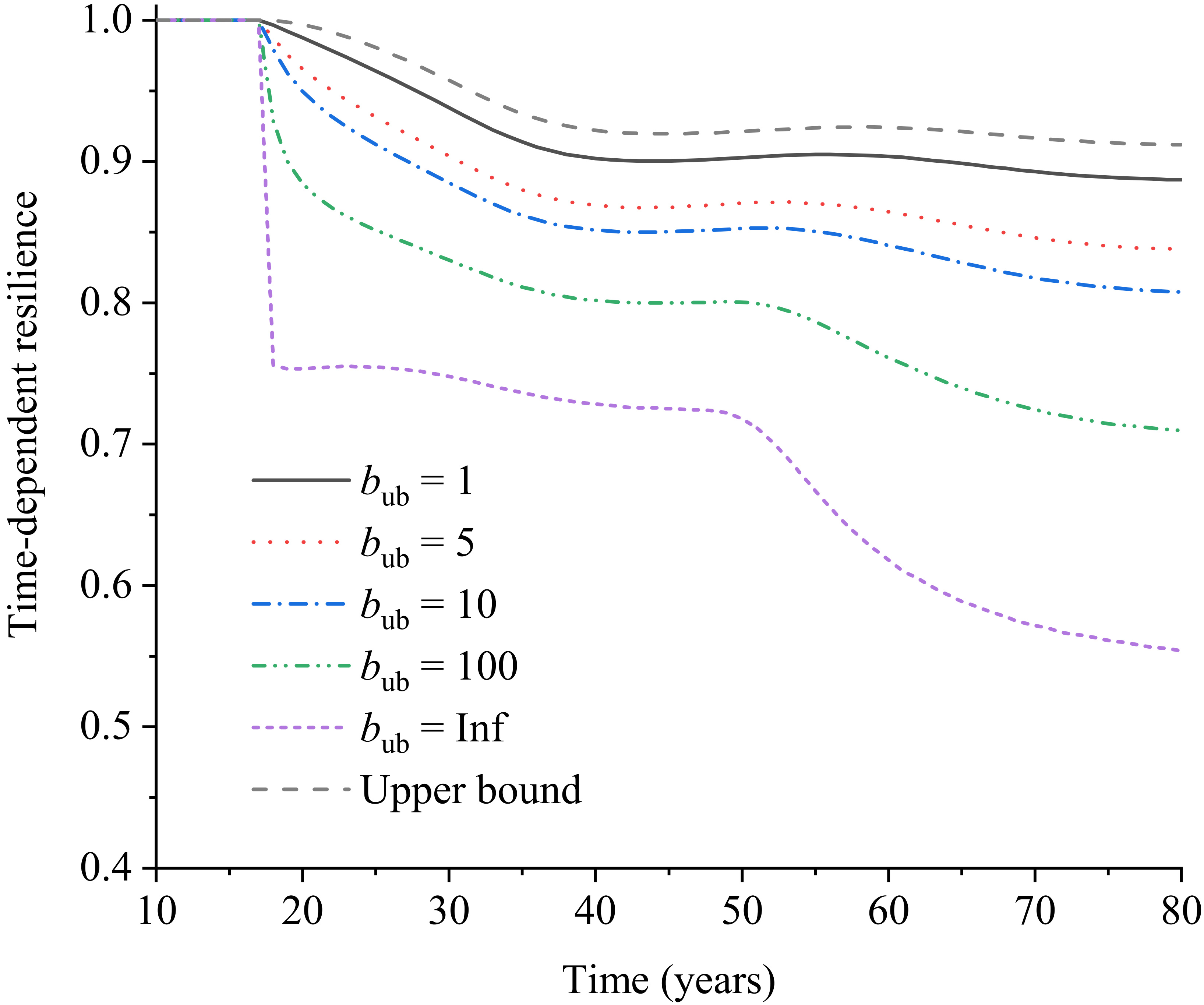
Time-dependent resilience
1.0
0.9
0.8
0.7
0.6
0.5
0.4
10
20
30
40
50
60
70
80
Time (years)
b_{ub} = 1
b_{ub} = 5
b_{ub} = 10
b_{ub} = 100
b_{ub} = Inf
Upper bound

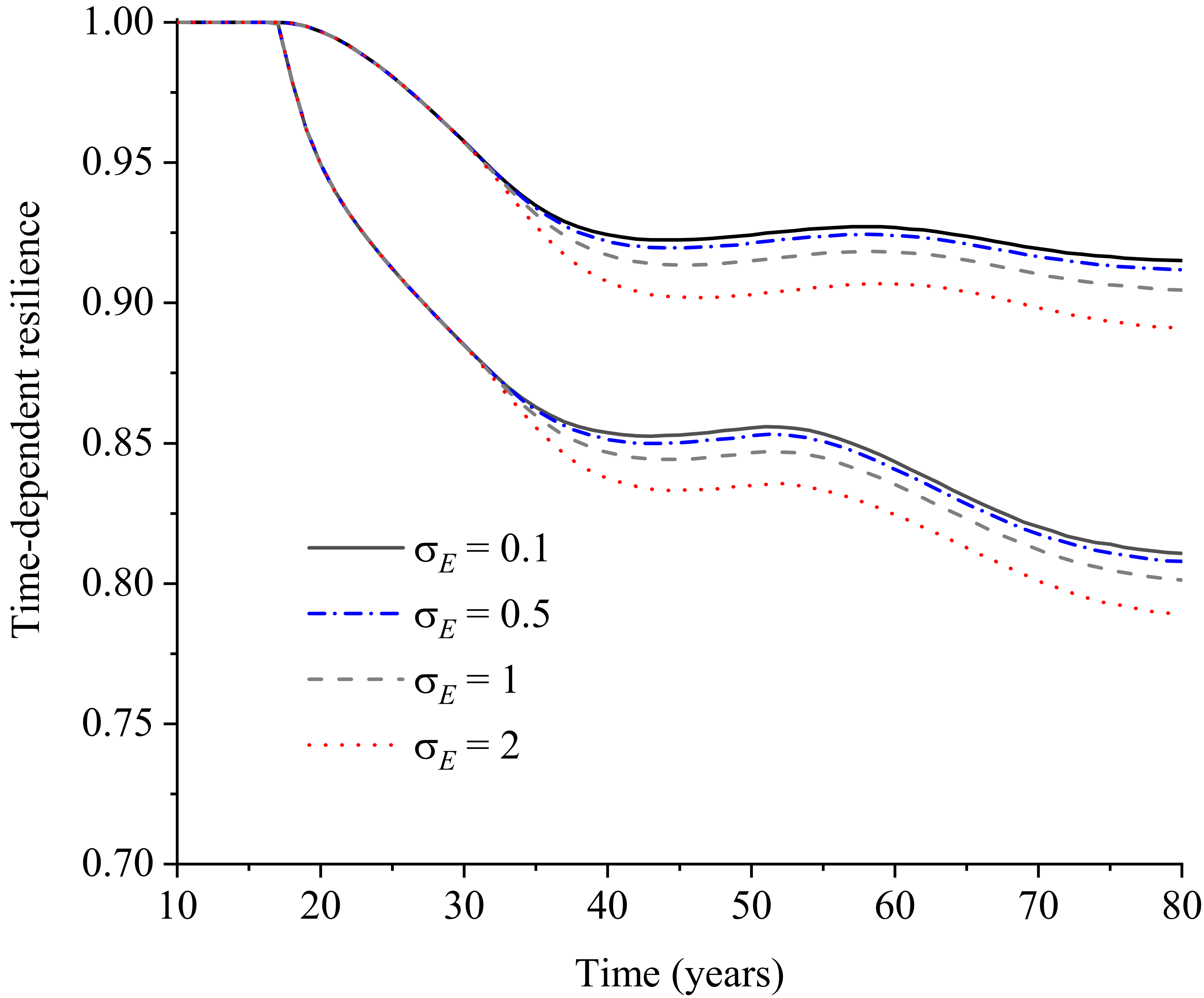
1.00
0.95
0.90
0.85
0.80
0.75
0.70
Time-dependent resilience
10
20
30
40
50
60
70
80
Time (years)
$\sigma_E = 0.1$
$\sigma_E = 0.5$
$\sigma_E = 1$
$\sigma_E = 2$